SENSITIVITY TO PREDATOR RESPONSE FUNCTIONS IN THE CHEMOSTAT

DEMONSTRATING THE SENSITIVITY OF CHEMOSTAT PREDATOR-PREY SYSTEMS TO THE FUNCTIONAL FORM OF HOLLING TYPE II PREDATOR RESPONSE FUNCTIONS

By
BRYDON EASTMAN, B.Sc.

A Thesis
Submitted to the School of Graduate Studies
in Partial Fulfillment of the Requirements
for the Degree
Master of Science

McMaster University

MASTER OF SCIENCE (2017)	McMaster University
(Mathematics)	Hamilton, Ontario

TITLE:	Demonstrating the Sensitivity of Chemostat Predator-Prey Systems to the Functional Form of Holling Type II Predator Response Functions
AUTHOR:	Brydon Eastman, B.Sc. (Redeemer University College, Canada)
SUPERVISOR:	Dr. Gail Wolkowicz
NUMBER OF PAGES:	69

Abstract

Biological models of predator-prey interaction have been shown to have high sensitivity to the functional form of the predator response (see [3]). Chemostat models with competition have been shown to be robust under various forms of response function (see [15]). The fcus here is restricted to a simple chemostat model with predator-prey dynamics. Several functional responses of Holling Type II form are considered. The sensitivity of dynamics to our choice of functional form is demonstrated by way of bifurcation theory. These results should be a warning to modelers, since by data collection and curve-fitting alone it is impossible to determine the exact functional form of the predator response function.

Acknowledgements

I would like to express my sincere gratitude to my supervisor Dr. Gail Wolkowicz for her many insightful comments, continued encouragement, and invaluable insight in the direction of this thesis. Further I would like to express my appreciation to my fiancée Tabitha for putting up with me when I only had head-space for research. I would be remiss without acknowledging my research group Tedra Bolger, Madeleine Hill, and Savannah Spilotro for the many late nights spent studying. I would also like to thank McMaster University for providing me this opportunity to pursue a subject that makes my heart sing and to all the funding sources for helping me stay fed while doing so. Lastly, to everyone who provided me coffee over the past two years without whom this thesis may never have been completed.

Table of Contents

List of Figures

Chapter 1

Introduction

1.1 Motivation

Predator-prey models have been widely used in ecology, epidemiology, and economics. These models are often based on the classical Lotka-Volterra equations (see, for example, [9]) or their extension in the Rosenzweig-MacArthur models [11]. In the Rosenzweig-MacArthur models the prey nullcline has at most one local extremum in the first quadrant. In any biological model there are parameters that correspond to biological properties of the particular systems being described. A standard procedure in analysing these models is to describe the qualitative changes in predictions elicited by quantitative changes in parameter values.

These predator-prey models all share a function called the predator-response function which describes the intake rate the predator adopts in response to the prey density. Typically the analytical form of this function is determined by taking any number of standard functions and fitting this function to experimental data in a least-squares problem. In a recent paper by Fussman and Blasius [3] it was shown that an extension of the predator-prey model due to Rosenzweig and MacArthur [11] is highly susceptible to

choice of response function. The authors of [3] demonstrate that under various response functions the predator-prey model may elicit a prey nullcline with two local extrema in the first quadrant. The main result of [3] demonstrates that two predator response functions that both describe the same shape can predict qualitatively different behaviour in the model (see Figure 1.1). This particular sensitivity was later described from a bifurcation theory perspective in a subsequent paper by Wolkowicz and Seo [13].

In practice, a modeler applying a particular predator-prey model will need to determine numerical values of multiple parameters related to the response of the predator to density of the prey population. To do so, a modeler may experimentally obtain multiple data points and fit some standard curve – via a least-squares procedure, or something similar – to these data points. If there is no biological motivation for a particular functional form of the predator response function external to the shape of the data, then any number of particular functional forms can be chosen. When considering experimental error, the fit of any particular functional form to the data may be indistinguishable from the fit of another. In Figure 1.1 this can be pictured. The figure focuses on four particular functional forms (that are precisely defined in Section 1.4) that have the same qualitative shape and perform comparably well under least-squares fitting to the simulated data. The plot of Monod and Arctan most closely fit the data. In Chapter 4, it will be demonstrated that these two functional forms will predict an entirely different sequence of bifurcations in the model and, as a result, a model where Arctan is used as a predator response function may make drastically different predictions than a model that uses Monod as the predator response function.

These results raise a natural question: is the sensitivity to response function choice a result specific to the generalised Rosenzweig-MacArthur models studied by [3] or does it apply to other predator-prey models as well? It is natural to ask if a more robust predator-prey model can be produced that

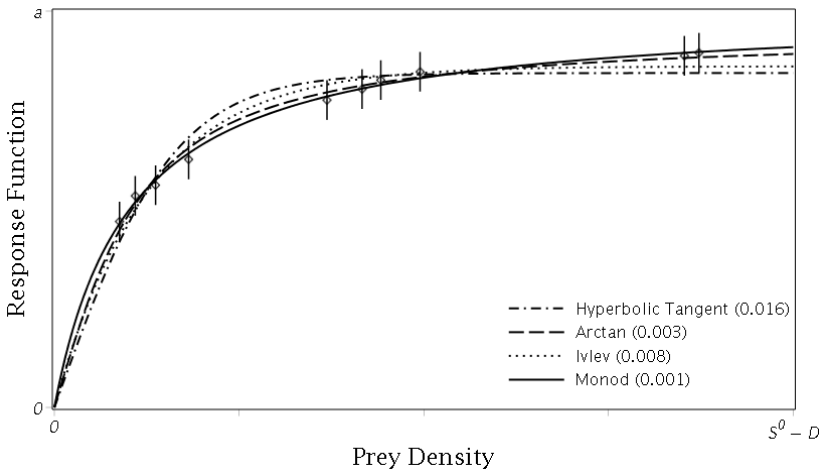

Figure 1.1: This plot was generated by sampling 10 uniformly distributed x values between 0 and $S^0 - D$. The y values were obtained by applying the map $x \to \frac{x}{1+x}$ and perturbing the result by a uniformly distributed random number between -0.025 and 0.025 (to simulate measurement error). The plots are then the Monod, Ivlev, Hyperbolic Tangent, and Arctan functions fit via least-squares in the parameters a and b, with the residuals recorded in the legend.

will be less sensitive to response function choice.

1.2 The Chemostat

The chemostat is a laboratory apparatus frequently used in microbial biology and lake ecology. It is a useful model for describing microbial growth under limited nutrient uptake in a highly controlled environment. These simple models are robust enough to make meaningful predictions, to a degree, about some of the population interactions present in complicated systems such as a lake.

The simpler forms of these models consider three chambers: a nutrient

reservoir, a growth chamber, and a discharge chamber. The fluid from the nutrient reservoir is pumped into the growth chamber at a constant rate where it is mixed well. The fluid from the growth chamber, along with any nutrients or microorganisms, is pumped out at the same rate into the discharge chamber.

Many articles have studied the chemostat from a modeling perspective. Wolkowicz and Lu [15] considered a chemostat model where various microorganisms competed in the growth chamber amongst each other for the limiting nutrient. The authors demonstrated the robustness of their model to various choice of response function in the competitive chemostat.

We consider a system where a population lives in the growth chamber that feeds on the nutrient being pumped in. We also consider a predator population in the same growth chamber that feeds off the prey. We investigate whether this model is just as structurally sensitive as the Rosenzweig-MacArthur model to choice of predator response functions, as in [3].

1.3 The Model

Let $s(t)$ denote the concentration of the nutrient in the growth chamber at time t and let $x(t)$ and $y(t)$ denote the density of prey and predator populations in the growth chamber at time t, respectively. The interactions of these three quantities are described by the following autonomous differential equations:

$$\begin{cases} \dot{s} = D\,(S^0 - s) - x\,p(s) \\ \dot{x} = x\,(\gamma p(s) - D) - y\,a\,q(bx) \\ \dot{y} = y\,(-D + \delta a\,q(bx)) \end{cases} \tag{1.1}$$

where D and S^0 are positive constants representing dilution and saturation of the limiting nutrient, respectively. The function $p(s)$ describes the benefit for a prey-organism to consume the nutrient and $\gamma > 0$ is the yield constant for

this nutrient uptake. Similarly, $q(x)$ represents the response of the predator to prey density and $\delta > 0$ is a yield constant. The positive parameters a and b are used in least-squares fitting to fit the functional form of $q(x)$ to experimentally obtained data (see Figure 1.1).

System (1.2) is a highly simplified system. In particular, notice that the model assumes that the species specific death rates are all the same.

Many different forms of p and q could be chosen. For the purpose of this thesis we take p to be described by mass-action, $p(s) = m\,s$ so that the benefit for a prey-organism to consume the limiting nutrient grows linearly with the amount of nutrient they consume. The exact functional form of $q(x)$ will be discussed in Section 1.4.

System (1.1) has seven unknown parameters all corresponding to some biological quantity. However, for the ease of analysis, we can change the units of our four dimensions (time (t), nutrient (s), prey organism (x), and predator organism (y)) to scale out four of the parameters in the model. Consider the following change of variables

$$\tilde{t} = \tfrac{m}{b}t, \quad \tilde{s} = b\gamma s, \quad \tilde{x} = bx, \quad \tilde{y} = \tfrac{b}{\delta}y$$

and the following rescaling of parameters

$$\tilde{S^0} = b\gamma S^0, \quad \tilde{D} = \tfrac{b}{m}D, \quad \tilde{a} = \tfrac{b\delta}{m}a.$$

A simple application of the chain rule yields

$$\begin{aligned}\frac{\mathrm{d}\tilde{s}}{\mathrm{d}\tilde{t}} &= \frac{\mathrm{d}\tilde{s}}{\mathrm{d}s}\frac{\mathrm{d}s}{\mathrm{d}t}\frac{\mathrm{d}t}{\mathrm{d}\tilde{t}} = \frac{\gamma b^2}{m}\dot{s}(\tilde{t}) \\ &= \frac{b}{m}D\left(b\gamma S^0 - b\gamma s\right) - bxb\gamma s \\ &= \tilde{D}\left(\tilde{S^0} - \tilde{S}\right) - \tilde{x}\tilde{s}.\end{aligned}$$

Similarly, for x and y.

$$\begin{aligned}\frac{\mathrm{d}\tilde{x}}{\mathrm{d}\tilde{t}} &= \frac{\mathrm{d}\tilde{x}}{\mathrm{d}x}\frac{\mathrm{d}x}{\mathrm{d}t}\frac{\mathrm{d}t}{\mathrm{d}\tilde{t}} = \frac{b^2}{m}\dot{x}(\tilde{t}) \\ &= \frac{b^2}{m}\left(x(\gamma m s - D) - y\,a', q(bx)\right) \\ &= bx\left(b\gamma s - \frac{b}{m}D\right) - b\delta y\frac{b}{m\delta}a\,q(bx) \\ &= \tilde{x}\left(\tilde{s} - \tilde{D}\right) - \tilde{y}\tilde{a}q(\tilde{x})\end{aligned}$$

$$\begin{aligned}\frac{\mathrm{d}\tilde{y}}{\mathrm{d}\tilde{t}} &= \frac{\mathrm{d}\tilde{y}}{\mathrm{d}s}\frac{\mathrm{d}y}{\mathrm{d}t}\frac{\mathrm{d}t}{\mathrm{d}\tilde{t}} = \frac{b^2}{m\delta}\dot{y}(\tilde{t}) \\ &= \frac{b^2}{m\delta}y\left(\delta a q(bx) - D\right) \\ &= \frac{b}{\delta}y\left(\frac{b}{m}\delta a q(bx) - \frac{b}{m}D\right) \\ &= \tilde{y}\left(\tilde{a}q(\tilde{x}) - \tilde{D}\right)\end{aligned}$$

For convenience, henceforth we drop the tildes in the notation of s, x, y, t and a, D, S^0.

Hence, System (1.1) is equivalent to the following non-dimensionalised system:

$$\begin{cases}\dot{s} = D\left(S^0 - s\right) - xs \\ \dot{x} = x\left(s - D\right) - a\,y\,q(x) \\ \dot{y} = y\left(a\,q(x) - D\right)\end{cases} \tag{1.2}$$

where the three parameters S^0, D, and a are all positive. While this change of units has resulted in a more parsimonious model that will be easier to analyse, the parameters S^0 and D are now only proportional to their original biological interpretation.

1.4 Predator Response Function

Following the work of Holling [7], modelers have used three main forms to describe response functions in predator-prey models. Holling Type I refers to a mass-action response function like $p(s)$ in System 1.2. Previously, many authors have referred to the function

$$\frac{a\,x}{1+b\,x} \tag{1.3}$$

as the Holling Type II response. We consider multiple functions that have the same qualitative shape as (1.3). The next definition captures the key properties of (1.3) that we concern ourselves with.

Definition 1.4.1. A function $q(x)$ is called *Holling Type II* if

1. $q(x) \in C^2([0,\infty])$,
2. $q(0) = 0$,
3. $q'(x) > 0$ for all $x > 0$,
4. $q''(x) < 0$ for all $x > 0$,
5. and $\lim_{x\to\infty} q(x) < \infty$.

For the purpose of this thesis, we consider four main forms of the predator-response function $q(x)$, all of which are "Holling Type II", in the sense that they satisfy Definition 1.4.1.

$$\begin{aligned} q_M(x) &\triangleq \frac{x}{1+x}, \\ q_I(x) &\triangleq 1 - e^{-x}, \\ q_A(x) &\triangleq \frac{2}{\pi}\arctan(x), \text{ and} \\ q_H(x) &\triangleq \tanh(x). \end{aligned}$$

We refer to these functions as Monod (q_M), Ivlev (q_I), Arctan (q_A), and Hyperbolic Tangent (q_H). Any function that satisfies Definition 1.4.1 has a horizontal asymptote. For convenience, henceforth we will consider, without loss of generality, all response functions q to be scaled so that

$$\lim_{x\to\infty} q(x) = 1.$$

The following Lemma follows directly from Definition 1.4.1, but will be useful in later analysis of System (1.2).

Lemma 1.4.1. *Let q satisfy the conditions of Definition 1.4.1, then $q(x) - xq'(x) > 0$ for all $x > 0$.*

Proof. Let q satisfy the conditions of Definition 1.4.1 and define $P(x) \triangleq q(x) - xq'(x)$. By Definition 1.4.1, $q(0) = 0$ and $q''(x) < 0$ for all $x > 0$. Hence, $P(0) = 0$ and $P'(x) = -xq''(x) > 0$ for all $x > 0$ and the Lemma follows. □

Chapter 2

Preliminary Results

In this chapter we will discuss the biological wellposedness of System (1.2), derivation and local stability analysis of the equilibria, and some preliminary analysis of the qualitative shape of the nullclines under various response functions.

Theorem 2.0.1. *There exists a unique solution* $(s(t), x(t), y(t))$ *that satisfies the vector field of System (1.2) under the initial conditions* $(s(0), x(0), y(0)) = (s_0, x_0, y_0) \in \mathbb{R}^3$.

Since the vector field described in System (1.2) is C^1, the theorem follows immediately.

For biological systems it is important to ensure that solution curves of the differential equations stay biologically relevant. In the case of System (1.2) this amounts to ensuring the solutions are bounded above and contained within the first octant.

2.1 Nonnegativity and Boundedness of Solutions

First let $u = s + x + y$, then it is a straightforward calculation to see that

$$\dot{u} = \dot{s} + \dot{x} + \dot{y} = -D\,(u - S^0). \tag{2.1}$$

Lemma 2.1.1. *Given non-negative initial data, the solutions of System (2.1) remain non-negative and bounded for all positive t and $u(t)$ converges to S^0 as $t \to \infty$.*

Proof. Assume $u(0) = u_0 \geq 0$. System (2.1) is a separable linear differential equation and can be integrated immediately to obtain

$$u(t) = \left(u_0 - S^0\right) e^{-Dt} + S^0.$$

Now,

$$u'(t) = \ D(S^0 - u_0)e^{-Dt} \quad \text{and} \quad u''(t) = \ -D^2(S^0 - u_0)e^{-Dt}$$

hence, if $u_0 = S^0$, then $u(t) = S^0$ for all $t \geq 0$. Likewise, if $u_0 < S^0$, then $u(t)$ increases to S^0 for all $t \geq 0$ and for $u_0 > S^0$, then $u(t)$ decreases to S^0 for all $t \geq 0$. □

Lemma 2.1.1 demonstrates that given non-negative initial conditions $s(0)$, $x(0)$, and $y(0)$, the System (1.2) converges to the plane $s(t)+x(t)+y(t) = S^0$. The sum of these three quantities (s, x, y) remains non-negative. Since these three variables each correspond to a biological quantity, we must show that individually they all remain non-negative.

Theorem 2.1.1. *Given $s(0) > 0$, $x(0) > 0$, and $y(0) > 0$ the solutions of the System (1.2) remain non-negative and bounded for all positive t.*

Proof. Assume $s(0) > 0$, $x(0) > 0$, and $y(0) > 0$ and let $(s(t), x(t), y(t))$ be solutions to System (1.2). The $(s, 0, y)$-plane (and the $(s, x, 0)$-plane) is invariant with respect to System (1.2), hence, by Theorem 2.0.1, any solution with $x(0) > 0$ (respectively $y(0) > 0$), cannot reach the plane in finite time. Therefore, given $x(0) > 0$ (respectively $y(0) > 0$), $x(t) > 0$ (respectively $y(t) > 0$) for all positive t. Furthermore, suppose there exists some $t_* > 0$ such that $s(t_*) = 0$. Then $\dot{s}(t_*) = S^0 D > 0$, a contradiction. Hence, given $s(0) > 0$, $s(t)$ is always positive. By Lemma 2.1.1, the sum of the solutions is non-negative and finite, moreover, $(s(t), x(t), y(t))$ individually are non-negative, and so the theorem follows. □

Theorem 2.1.1 allows us to consider a reduced system of differential equations. This theorem suggests that any solution curves to System (1.2) eventually converge to the simplex governed by $s + x + y = S^0$ contained entirely in the first octant. Hence, we can reformulate this three-dimensional system as a two dimensional system in x, y space.

Evaluating the time derivative of x from System (1.2), we observe.

$$\begin{aligned} \dot{x} &= x\,(s - D) - a\,y\,q(x)\big|_{s=S^0-x-y} \\ &= x\,(S^0 - x - y - D) - a\,y\,q(x) \end{aligned}$$

Hence, we are left with the following system, which is equivalent to System (1.2) evaluated on the simplex $s + x + y = S^0$ contained in the first octant.

$$\begin{cases} \dot{x} = & x\,(S^0 - D - x) - y\,(a\,q(x) + x) \\ \dot{y} = & y\,(a\,q(x) - D) \end{cases} \tag{2.2}$$

See Figure 2.1 for an example of two trajectories, one for the 3D System (1.2) and one for the 2D System (2.2). Note that the qualitative behaviour of each trajectory is the same and how quickly the trajectory in the 3D system converges to the simplex $s + x + y = S^0$. Any solution $(x(t), y(t))$ of the two dimensional System (2.2) corresponds to solutions of the three dimensional

System (1.2) that lie on the simplex $s + x + y = S^0$ embedded in (s, x, y)-space. By Lemma 2.1.1, any solution of System (1.2) converges exponentially to this simplex. The omega limit set of any trajectory of System (1.2) lies on this simplex. Hence, there is a bijective correspondence between equilibria of each system. Assume $(\bar{x}, \bar{y})$ is an equilibrium of System (2.4). Then $(S^0 - \bar{x} - \bar{y}, \bar{x}, \bar{y})$ is an equilibrium of System (1.2) (moreover, if $(\tilde{s}, \tilde{x}, \tilde{y})$ is an equilibrium of System (1.2), then $(\tilde{x}, \tilde{y})$ is an equilibrium of System (2.2) and, by Lemma 2.1.1, $\tilde{s} + \tilde{x} + \tilde{y} = S^0$). Any equilibrium of System (2.2) has the same local stability as the corresponding equilibrium of System (1.2). This follows since solution curves of System (1.2) converge exponentially to the $s+x+y = S^0$ simplex, by Lemma 2.1.1, hence, the additional eigenvalue in the three dimensional case is necessarily negative. Since the boundary of the simplex is either invariant ($x = 0$ or $y = 0$) or repelling into the interior of the simplex ($s = 0$), those points in the omega limit set of a trajectory of System 1.2 that lie on the boundary of the simplex and the positive octant cannot belong to a periodic orbit. Hence, any periodic orbit of System 1.2 is contained entirely in the interior of the simplex $s + x + y = S^0$. All that is left to justify is that the global dynamics of the systems are equivalent. To do so we show that System (1.2) satisfies all the hypotheses of the convergence theorem in [14]. This proves that when an equilibrium is globally asymptotically stable in System (2.2), it is also globally asymptotically stable in System (1.2). This theorem and its proof are left until Appendix A in Theorem A.1.

The preceding theorems have allowed us to eliminate a dimension from System (1.2). This is an important result, since planar systems are significantly less complex than higher dimensional systems (in particular, familiar theorems like Poincaré-Bendixson are now applicable for the reduced, planar system). The choice to eliminate the s dimension may seem arbitrary, but we are primarily concerned with investigating the sensitivity of predator-prey

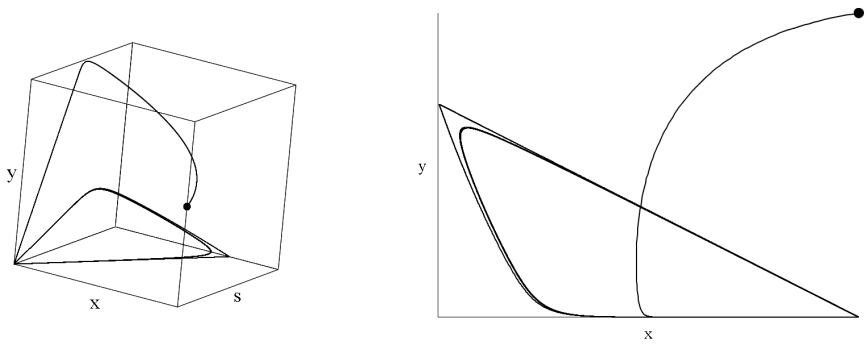

Figure 2.1: Figure illustrating trajectories in the 3D system (1.2) compared to those in the 2D system (2.2). The filled circle represents the starting point of the trajectory. In both systems the trajectory converges to a large periodic orbit.

systems in the chemostat under Holling Type II response function choice and comparing this to the previously observed sensitivity in Rosenzweig-MacArthur predator-prey systems. For this exact reason, eliminating s (the nutrient) and keeping x (the prey) and y (the predator) in the model is entirely natural.

A consequence of the above theorems allows us to state the following theorem that follows immediately from Theorem 2.1.1.

Theorem 2.1.2. *The solutions of System (2.2) with non-negative initial data are bounded and remain non-negative for all positive time.*

2.2 Preliminary Analysis of the Prey Nullcline

The first equation in System (2.2) yields two nullclines. The first corresponds to prey extinction, $x = 0$. The second is given by

$$y = F(x) \triangleq x\frac{S^0 - D - x}{x + a\,q(x)}. \tag{2.3}$$

This second nullcline is the only one with any hope of eliciting an equilibrium point interior to the first quadrant. For this reason we often refer to it as *the* prey nullcline.

This formulation allows us to rewrite System (2.2) more compactly.

$$\begin{cases} \dot{x} &= (F(x) - y)(a\,q(x) + x) \\ \dot{y} &= y(a\,q(x) - D) \end{cases} \tag{2.4}$$

The prey nullcline and its qualitative shape will end up being a very important component for evaluating the sensitivity of these models to response function choice. For that very reason we will now take the time to make some preliminary analysis of the prey nullcline.

We extend the definition of $F(x)$ to include $F(0)$ in the standard way. A simple application of L'Hôpital's Rule yields:

$$F(0) \triangleq \lim_{x\to 0} F(x) = \frac{S^0 - D}{1 + a\,q'(0)}.$$

Similarly, two applications of L'Hôpital's Rule yields:

$$F'(0) \triangleq \lim_{x\to 0} F'(x) = -\frac{a\,q''(0)(S^0 - D) + 2a\,q'(0) + 2}{2(1 + q'(0))^2}.$$

Now $F(S^0 - D) = 0$. For this reason we may often make use of the shorthand $K = S^0 - D$ (hence, $F(K) = 0$).

The prey nullcline $F(x)$ depends on three parameters, S^0, D, and a. However, as we will see in Chapter 4 the parameter S^0 is an important parameter

in observing dynamical changes. For this reason, we may refer to $F(x;S^0)$ to refer to the function $F(x)$ parameterised by some particular S^0. Note that in these cases, primes should always be interpreted as x-derivatives (i.e. $F'(x;S^0) \triangleq \partial_x F(x;S^0)$).

The derivative of the prey nullcline, $F'(x;S^0)$, is linear in S^0. Hence, it is possible to find an expression $S^0(x)$ such that $F'(x;S^0(x)) = 0$ for all x. In particular,

$$F'(x;S^0) = \frac{a\,x(d+x)q'(x) - a\,(d+2x)q(x) - x^2 + a\,(q(x) - xq'(x))S^0}{(a\,q(x)+x)^2}$$

Hence,

$$S^0(x) \triangleq \frac{(1+a\,q'(x))x^2 + aD(q(x) - xq'(x)) + 2xa\,q(x)}{a(q(x) - xq'(x))} \tag{2.5}$$

Notice that by Lemma 1.4.1 we have that $S^0(x) > 0$ for all $x > 0$.

This formulation of $S^0(x)$ allows us to choose an S^0 for some fixed value of x, say $\bar{x}$, where

$$F'(\bar{x};S^0(\bar{x})) = 0.$$

Note that (2.5) guarantees that for *any* predator response function $q(x)$ we can fix our parameter S^0 to guarantee at least one positive local extremum of the prey nullcline for positive x. Later on we will see that counting the number of positive extrema for the prey nullcline is very important for determining all possible dynamics.

These basic properties lead us to the following obvious remarks about the qualitative shape of the prey nullcline.

Remark 2.2.1. *If $S^0 < D$, then $F(x) < 0$ for all positive x.*

This observation is due to the fact that $F(x)$ has one root at $x = S^0 - D$, and the sign of $F(0)$ is entirely determined by the sign of $S^0 - D$. A trivial application of the intermediate value theorem achieves the remark.

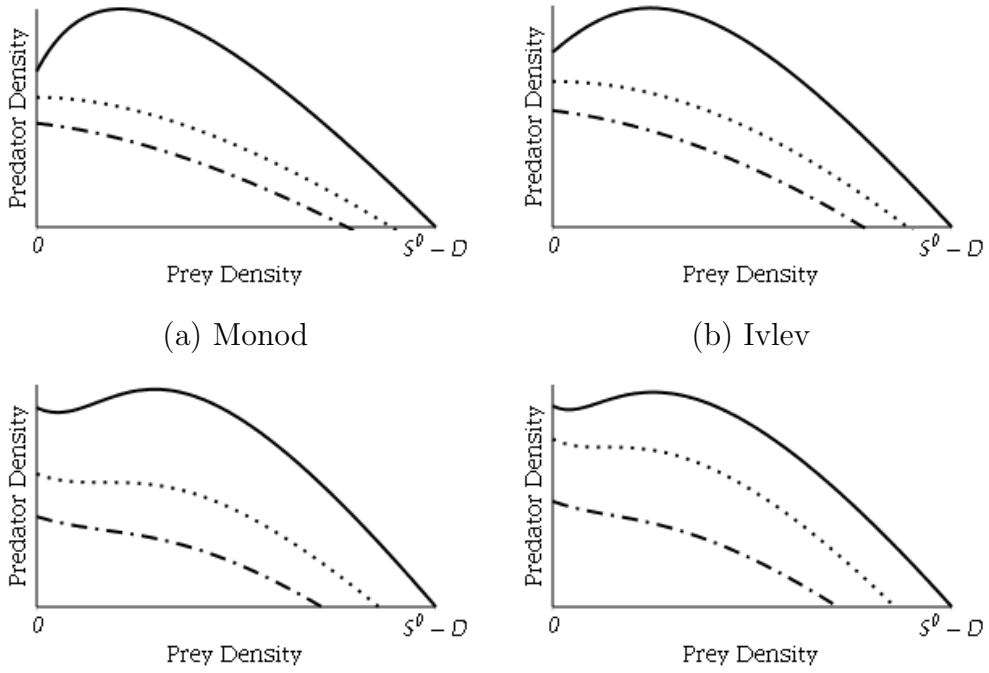

(a) Monod (b) Ivlev

(c) Hyperbolic Tangent (d) Arctan

Figure 2.2: Plots demonstrating the qualitative shape of the prey nullcline under various response functions. The solid curve indicates the prey nullcline with the maximum number of local extrema, the dotted curve indicates when the prey nullcline is strictly non-increasing, and the dash-dot curve when the prey nullcline is strictly decreasing.

Remark 2.2.2. *If $S^0 > D$, then $F'(S^0 - D) < 0$.*

Remark 2.2.3. *If $S^0 > D$, then $F(x)$ has one positive root and $F(x) > 0$ for $0 \leq x < S^0 - D$.*

We have already observed the importance of $S^0 - D$ as the root of the prey nullcline, but now we are characterising more carefully the intervals of potential interest. Any biologically relevant equilibrium point involving the prey nullcline must take place on this finite interval $0 \leq x \leq S^0 - D$. Therefore, any equilibrium in the interior of the first quadrant must lie in this interval.

Remark 2.2.4. *If $q(x) = q_A(x)$ or $q(x) = q_T(x)$, then $F'(0) < 0$.*

Remark 2.2.4 is true for all Holling Type II functions for which $q''(0) = 0$ (of which Arctan and Hyperbolic Tangent are, but two examples). This is particularly interesting to observe since it is not always true in the Monod and Ivlev cases. Both the Monod and Ivlev response functions can induce a prey nullcline with arbitrarily signed slope at $x = 0$. This is the first main difference between the qualitative shapes of the prey nullcline for various Holling Type II response functions. Moreover, Remark 2.2.4 and Remark 2.2.2 characterise the behaviour of the slope of the prey nullcline at the boundaries of the biologically relevant x values.

2.3 Local Stability Analysis

Similarly, we can investigate the two nullclines yielded by the second equation in System (2.4). Namely, $y = 0$ and $x^* \triangleq q^{-1}(D/a)$. Since $q(x)$ increases from 0 asymptotically to 1, the existence of x^* is guaranteed if, and only if, $a > D$.

Thus System (2.4) has at most three biologically relevant equilibrium points:

$$E_{ME} = (0,0), \quad E_I = (x^*, F(x^*)), \quad E_E = (S^0 - D, 0)$$

(where E_{ME} is mutual extinction of both the predator and prey, E_I is an interior equilibrium corresponding to coexistence of the predator and prey, and E_E is the extinction of the predator).

Linearising System (2.4) about each equilibrium point yields the following Jacobian matrices:

$$J_{ME} = \begin{bmatrix} F(0)(aq'(0)+1) & 0 \\ 0 & -D \end{bmatrix}$$

$$J_I = \begin{bmatrix} F'(x^*)(D+x^*) & -(D+x^*) \\ a\,F(x^*)q'(x^*) & 0 \end{bmatrix}$$

$$J_E = \begin{bmatrix} F'(K)(a\,q(K)+K) & -(a\,q(K)+K) \\ 0 & a\,q(K)-D \end{bmatrix}$$

with eigenvalues that determine the local stability of each equilibrium point.

All these eigenvalues depend on the parameters S^0, a, D. We will consider all of the possible cases.

If $S^0 < D$ then, as seen in Remark 2.2.1, this implies $F(x) < 0$ for all $x > 0$. In this case the only equilibrium point in the first quadrant is E_{ME}. Since J_{ME} is diagonal, and $F(0) < 0$ for $S^0 < D$, we see that E_{ME} is locally stable for $S^0 < D$. From standard phase plane analysis it follows that E_{ME} is globally asymptotically stable for System (1.2).

If $S^0 > D$ we consider three sub-cases. Suppose $a \leq D$. Then the equilibrium point E_I does not exist and the only equilibrium points in the first quadrant are E_{ME} and E_E. In this case J_{ME} has two real eigenvalues of opposite sign and hence, E_{ME} is an unstable (saddle) equilibrium. The matrix J_E is upper-triangular and hence, its eigenvalues lie on the main

diagonal. Now $a \leq D$ implies that $a\,q(x) < D$ and hence, J_E has two negative eigenvalues. Thus E_E is a local asymptotically stable equilibrium point. Again from standard phase plane analysis it follows that E_{ME} is globally asymptotically stable for System (1.2).

Assume $S^0 > D$, $a > D$, and $x^* > K$. Again we see that E_I does not exist in the first quadrant. As in the previous case, one can see that J_{ME} has two eigenvalues of opposite sign and J_E has two negative eigenvalues (since $K < x^*$ and $q'(x) > 0$ for positive x implies that $a\,q(K) < a\,q(x^*) = D$). Hence, in this case as well we observe that E_{ME} is unstable (saddle) and E_E is locally asymptotically stable.

Lastly, assume $S^0 > D$, $a > D$, and $0 < x^* < K$. Now all three equilibria exist in the first quadrant. As in the previous cases with $S^0 > D$, we observe that J_{ME} has two eigenvalues of opposite sign, hence, E_{ME} is an unstable (saddle) equilibrium point. Since $x^* < K$ and $q'(x) > 0$ for positive x, we have that $a\,q(K) > D$. Hence, J_E also has two eigenvalues of opposite sign. Therefore, E_E is an unstable (saddle) equilibrium point as well. The coexistence equilibrium point proves more interesting. J_I has eigenvalues

$$\lambda_{I_{+,-}} = \frac{(D + x^*)}{2}\left(F'(x^*) \pm \sqrt{F'(x^*)^2 - \frac{4aF(x^*)q'(x^*)}{D + x^*}}\right). \tag{2.6}$$

Note that $(D + x^*) > 0$ and $4aF(x^*)q'(x^*) > 0$, since $x^* < K$ and $S^0 > D$. Hence, $F'(x^*)^2 - (4aF(x^*)q'(x^*))/(D + x^*) < F'(x^*)^2$. Therefore, the sign of the real part of either eigenvalue depends entirely on the sign of $F'(x^*)$. If $F'(x^*) < 0$, then both eigenvalues have negative real part and E_I is a local asymptotically stable equilibrium point. If $F'(x^*) > 0$, then both eigenvalues have positive real part and E_I is an unstable equilibrium point.

Chapter 3

Nullcline Analysis

In Chapter 2 we investigated the shape of the prey nullcline and determined the local stability of each equilibrium point. We observed that the stability of the interior equilibrium point depends on the slope of the prey nullcline at that point. In this chapter we will investigate the response function in more detail providing a condition for the exact number of extrema a response function can elicit in the prey nullcline (Section 3.1), we will characterise the number of inflection points in the prey nullcline (Section 3.2), and finally we will demonstrate how the locations of these extrema depend upon the bifurcation parameter S^0 (Section 3.3). By the end of this chapter the plot in Figure 2.2 will be justified as demonstrating all the qualitative shapes of the nullclines for Monod, Ivlev, Arctan, and Hyperbolic Tangent predator response functions.

Throughout this chapter, unless explicitly stated otherwise, it is assumed that $a > D$, $S^0 > D$, and $x^* < K$. In other words, it is assumed that the interior equilibrium exists in the first quadrant.

3.1 Response Function Stratification

In this Section we will establish conditions that determine the number of local extrema the prey nullcline can have in System (2.4) for various response functions.

Figure 3.1 depicts contour plots of the derivative of the prey nullcline in System (2.4) with the Arctan response function. One of the key realisations from Figure 3.1 is the recognition that varying a does not fundamentally change the shape of the plot. In fact, $K = S^0 - D$ is the only parameter that seems to influence the qualitative shape of the contour plot.

In Figure 3.1 the number of times the black curve crosses any horizontal line $K = \tilde{K}$ represents the number of positive zeros of $F'(x; \tilde{K})$. Similar to (2.5), we now derive an expression $\hat{K}(x)$ such that $F'(x; \hat{K}(x)) = 0$.

$$F'(x; K) = \frac{aK\left(q(x) - xq'(x)\right) + ax^2q'(x) - 2axq(x) - x^2}{(x + aq(x))^2}$$

The above equation demonstrates that $F'(x; K)$ is linear in K, so we can solve $F'(x; \hat{K}) = 0$ for $\hat{K}$ to obtain the expression

$$\hat{K}(x) \triangleq \frac{x\left(2aq(x) - axq'(x) + x\right)}{a\left(q(x) - xq'(x)\right)}.$$

In Figure 3.1, $\hat{K}(x)$ describes the solid black curve. We are concerned with the fundamental shape of $\hat{K}(x)$, in particular we are concerned with the maximum number of times any horizontal line can cross the curve for any particular choice of response-function $q(x)$; this represents the maximum number of local extrema in the prey nullcline. To this end, we investigate the first derivative of $\hat{K}(x)$ for the purpose of finding its critical points.

$$\hat{K}'(x) = \frac{\left(x^2q''(x) + 2(q(x) - xq'(x))\right)(aq(x) + x)}{a\left(q(x) - xq'(x)\right)^2} \tag{3.1}$$

Since we only are concerned with the positive critical points of $\hat{K}(x)$ we can ignore the positive denominator and the positive factor $(aq(x) + x)$ in the

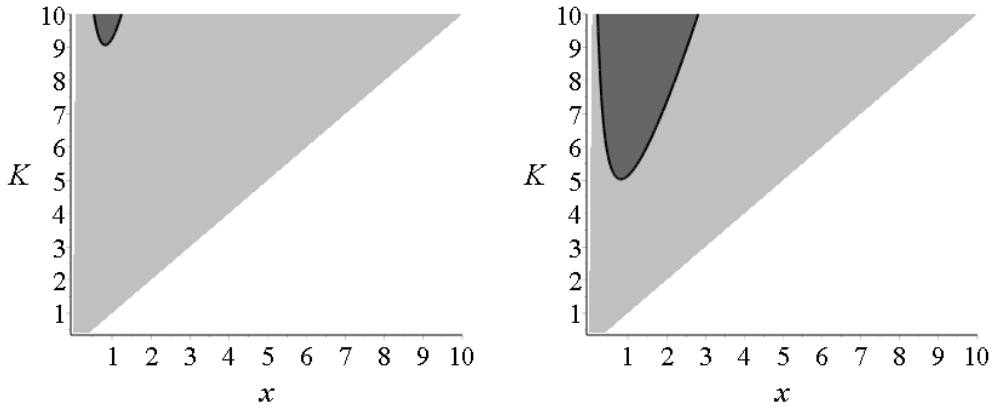

(a) $a = 1$

(b) $a = 4$

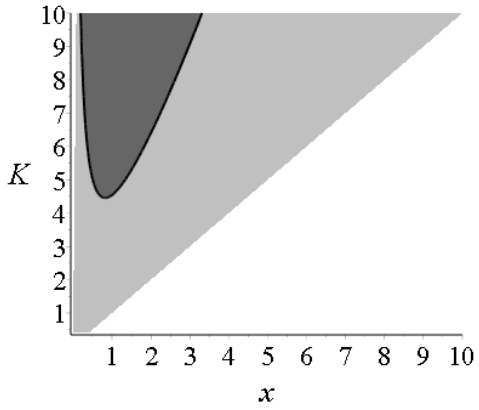

(c) $a = 7$

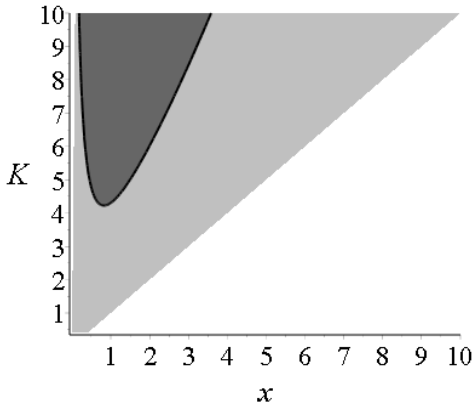

(d) $a = 10$

Figure 3.1: Contour plots of $F'(x; K)$ for the Arctan response function under various values of a with $0 \leq x \leq 10$ and $x < K \leq 10$. The black curve represents $F'(x; K) = 0$ (i.e. the function $\hat{K}(x)$), the light grey region represents negative $F'(x; K)$, and the dark grey region represents positive $F'(x; K)$.

numerator of equation (3.1).

$$H(x) \triangleq x^2 q''(x) + 2(q(x) - xq'(x)) \tag{3.2}$$

In effect, we have derived that $\hat{K}(x)$ has a positive critical point if, and only if, $H(x)$ has a positive root. This motivates the following theorem.

Theorem 3.1.1. *Consider the prey nullcline $F(x;K)$ obtained using some particular Holling Type II predator response function $q(x)$. If $H(x)$ has k positive roots, then $F(x)$ has at most $k+1$ positive local extrema.*

Proof. By definition of $H(x)$, $\hat{K}(x)$ has as many positive critical points as $H(x)$ has roots. Furthermore, by definition of $\hat{K}(x)$, every time $\hat{K}(x)$ crosses a horizontal line $K = \tilde{K}$ the function $F'(x;\tilde{K})$ has a zero.

It follows from the mean value theorem and mathematical induction that if there exists $(k+1)$ numbers $(x_1, \ldots, x_{k+1})$ such that $\hat{K}(x_i) = \tilde{K}$ for all $1 \leq i \leq (k+1)$, then there must be at least k critical points of $\hat{K}(x)$ between x_1 and x_{k+1}. The statement of the theorem follows. □

This theorem easily lends itself to determining the qualitative shape of the prey nullcline under various predator-response functions. For instance, consider the following example.

Corollary 3.1.1. *The prey nullcline (2.3) with Arctan predator response function has at most two local extrema.*

Proof. Consider expression $H(x)$ (from (3.2)) parameterised by $q(x) = q_A(x)$. Now $H'(x) = x^2 q'''(x)$, hence

$$\begin{aligned} H''(x) &= 2xq'''(x) + x^2 q^{(\mathrm{iv})}(x) \\ H'''(x) &= 2q'''(x) + 4xq^{(\mathrm{iv})}(x) + x^2 q^{(\mathrm{v})}(x). \end{aligned}$$

(where $q^{(\mathrm{iv})}(x)$ and $q^{(\mathrm{v})}(x)$ are the fourth and fifth derivatives of q, respectively).

Hence, $H'(0) = H''(0) = 0$ and $H'''(0) = 2q'''(0) = -\frac{8}{\pi}$. Hence, H initially decreases. Now $H(1) = \frac{\pi-3}{\pi} > 0$. Furthermore,

$$H'(x) = \frac{4x^2}{\pi}\left(\frac{3x^2-1}{(x^2+1)^3}\right)$$

which has a unique positive root at $x = \frac{1}{\sqrt{3}}$. Hence, $H(x)$ has exactly one positive root, so by Theorem 3.1.1, the corollary follows. □

Similar proofs can show that the prey nullcline with $q = q_H$ has at most two local extrema. Similarly, when considering $q = q_M$ or $q = q_A$, the prey nullcline has at most one local extremum. The proofs of these corollaries are left until Appendix B, though they follow the same structure as Corollary 3.1.1.

Corollary 3.1.2. *The prey nullcline (2.3) with Hyperbolic Tangent response function has at most two local extrema.*

Corollary 3.1.3. *The prey nullcline (2.3) with Monod response function has at most one local extremum.*

Corollary 3.1.4. *The prey nullcline (2.3) with Ivlev response function has at most one local extremum.*

The important power of Theorem 3.1.1 is that the expression $H(x)$ is entirely parameter-free. So while for any particular function $q(x)$ it may be difficult to analytically count the number of roots of $H(x)$, in practice it is easy to just plot $H(x)$ and count the number of roots. Moreover, since the prey nullcline $F(x;K)$ is only non-negative for $0 \leq x \leq K$, one needs only to plot $H(x)$ over the finite domain $0 \leq x \leq K$.

Furthermore, this result dictates that the possible shapes of the prey nullcline for System (2.4) are entirely limited by the response function and not any of the parameters of the system. Those parameters merely transition the

prey nullcline through the possible number of local extrema, as determined by Theorem 3.1.1, but it is truly the choice of response function that dictates the possible forms the prey nullcline can take given certain parameter conditions.

3.2 Number of Inflection Points of the Prey Nullcline

The following lemma and theorem demonstrate that, for any particular response function, to determine the number of inflection points of the prey nullcline one must count the roots of the following, parameter free condition:

$$\eta(x) \triangleq x(q(x) - xq'(x))q'''(x) + \frac{3}{2}q''(x)(2(q(x) - xq'(x)) + x^2q''(x)).$$

Lemma 3.2.1. *If $\eta(x)$ has no roots, then $F(x)$ has at most one inflection point.*

Proof. To investigate the inflection points, we consider the second derivative of the prey nullcline

$$F''(x) = a\frac{2(q(x) - xq'(x))(aq(x) + S^0 - D + a(S^0 - D - x)q'(x))}{(a\,q(x) + x)^3} - a\frac{x(aq(x) + x)(S^0 - D - x)q''(x)}{(q(x) + x)^3}$$

which is linear in S^0. Hence, the equation $F''(x) = 0$ can be easily solved to produce a function $\tilde{S}^0(x)$ such that $F''(x; \tilde{S}^0(x)) = 0$ for all x.

In a contour plot of $F''(x; S^0)$ with S^0 on the vertical axis and x on the horizontal axis, $\tilde{S}^0(x)$ describes the null-contour. If $\tilde{S}^0(x)$ is always increasing (respectively, decreasing) then for any particular S^0 value there is at most one x value for which $F''(x; S^0) = 0$. Furthermore,

$$\frac{\mathrm{d}}{\mathrm{d}x}\tilde{S}^0(x) = \frac{2(x + aq(x))^2\eta(x)}{(x(x + aq(x))q''(x) + 2(q(x) - xq'(x))(1 + aq'(x)))^2}.$$

Therefore, $\frac{\mathrm{d}}{\mathrm{d}x}\tilde{S}^0(x) = 0$ for $x > 0$ if, and only if, $\eta(x) = 0$ and the statement of the Lemma follows. □

Theorem 3.2.1.

i. $F(x)$ *parameterised by* $q(x) = q_I(x)$ *has at most one inflection point*

ii. $F(x)$ *parameterised by* $q(x) = q_A(x)$ *has at most one inflection point*

iii. $F(x)$ *parameterised by* $q(x) = q_H(x)$ *has at most one inflection point*

Proof. ii. In the case of $q(x) = q_A(x)$,

$$\eta(x) = \frac{8x}{\pi^2(x^2+1)^4}p(x) \text{ with } p(x) \triangleq 3x^3 - 4x^2\arctan(x) - 4\arctan(x) + 4x.$$

For positive x the function $\eta(x) = 0$ if, and only if, $p(x) = 0$ for some $x > 0$. Firstly, $p(0) = 0$ and $p'(x) = x(9x - 8\arctan(x))$. Since $\arctan(x)$ is sub-linear (i.e. $\arctan(x) < x$ for all $x > 0$), $p'(x) > 0$. Hence, $p(x) > 0$ for all $x > 0$ so, by Lemma 3.2.1, the theorem follows.

The proofs for the other two cases are similar and have been left until Appendix C. □

For the response function $q_M(x)$ the prey nullcline has a different shape. In particular, when parameterised by $q(x) = q_M(x)$,

$$F''(x) = -2a\frac{a - D + S^0 + 1}{(a + 1 + x)^3} < 0$$

and hence, the prey nullcline has no inflection points and is concave down for all positive x.

3.3 Dependence of the Extrema Location on Parameters

It will be useful to understand how the qualitative shape of the prey nullcline changes as S^0 changes. In this section we determine the direction the local

extrema drift as S^0 increases. This drift is illustrated in Figure 3.2.

Theorem 3.3.1. *The pair $(x_M, F(x_M))$ corresponding to a local maximum of $F(x; S^0)$ moves up and to the right as S^0 increases. The pair $(x_m, F(x_m))$ corresponding to a local minimum of $F(x; S^0)$ moves up and to the left as S^0 increases.*

Proof. First let x_M and x_m be the locations of the local maximum and minimum of the prey nullcline (if they exist). Now,

$$\partial_{S^0} F(x; S^0) = \frac{x}{x + aq(x)}$$

which is positive for all positive x. Furthermore,

$$\partial^2_{x,S^0} F(x; S^0) \triangleq \partial_x \left(\partial_{S^0} F(x)\right) = \partial_x \left(\frac{x}{x + aq(x)}\right) = a\frac{q(x) - xq'(x)}{(x + aq(x))^2}$$

which, by Lemma 1.4.1, is also positive for all positive x.

Therefore, $F'(x; S^0)$ is an increasing function of S^0. In a neighbourhood of x_M, $F(x; S^0)$ is concave down and $F'(x_M; S^0) = 0$. Hence, if S^0 is slightly increased then $F'(x_M; S^0) > 0$ and, since $F(x; S^0)$ is concave down, the new maximum is slightly larger than x_M. Therefore, a local maximum (if one exists) moves to the right. Similarly, a local minimum (if one exists) moves to the left.

Also, F is an increasing function of S^0 for each fixed $x > 0$. Hence, the value of $F(x; S^0)$ at a local maximum (if one exists) moves up as S^0 increases. Let $\epsilon > 0$ and let x_1 and x_2 be the local minima of $F(x; S^0)$ and $F(x; S^0 + \epsilon)$ respectively. Then $F(x_1; S^0) < F(x_2; S^0)$, since x_1 is the local minimum of $F(x; S^0)$. Moreover, $F(x_2; S^0) < F(x_2; S^0 + \epsilon)$, since $\partial_{S^0} F > 0$. Hence, $F(x_1; S^0) < F(x_2; S^0 + \epsilon)$. Therefore, the local minimum moves up as S^0 increases. □

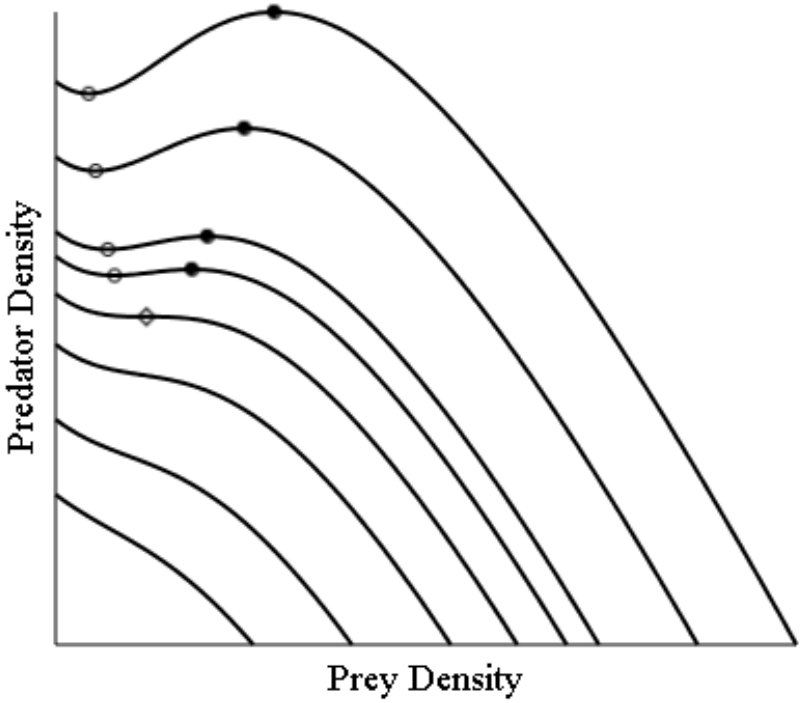

Figure 3.2: Figure illustrating the movement of the extrema as the parameter S^0 is increased. The figure was created by taking $q(x) = q_H(x)$. In each plot $(a, D) = (2, 1)$ and S^0 increases from 3 to 8.5. A hollow circle represents the position of the local minimum, a filled circle represents the position of the local maximum, and the diamond represents where the critical point and inflection point coincide.

Chapter 4

Bifurcation Analysis

In Section 2.3 we observed the existence of three equilibria, the mutual-extinction, prey extinction, and co-existence equilibria (denoted E_{ME}, E_E, and E_I respectively).

$$E_{ME} = (0, 0), \quad E_E = (S^0 - D, 0), \quad E_I = (x^*, F(x^*))$$

We now describe the sequence of bifurcations that System (2.4) undergoes as S^0 is increased from 0. This process involves considering parameter ranges that are not biologically relevant. The local stability of equilibria examined in Section 2.3 was not considered for these biologically irrelevant parameter spaces. Hence, we will also need to determine the stability of the equilibria for these parameter spaces in order to fully classify the bifurcations that occur. Before we begin we first highlight the following remarks:

- If $a \leq D$, then E_I does not exist.
- If $a > D$, then E_I does exist. However, x^* may be bigger than $S^0 - D$. If this is the case, then $F(x^*) < 0$ and so E_I is in the interior of the first quadrant (see Remark 2.2.2 and Remark 2.2.3).

- If $a > D$, then S^0 can be taken sufficiently large so as to ensure $S^0 - D > x^*$. Hence, if $a > D$, then S^0 can be taken large enough to ensure that E_I is in the interior of the first quadrant.

Figure 4.1 illustrates the following discussion in the case that $a = 2$, $D = 0.5$, and $q = q_A$.

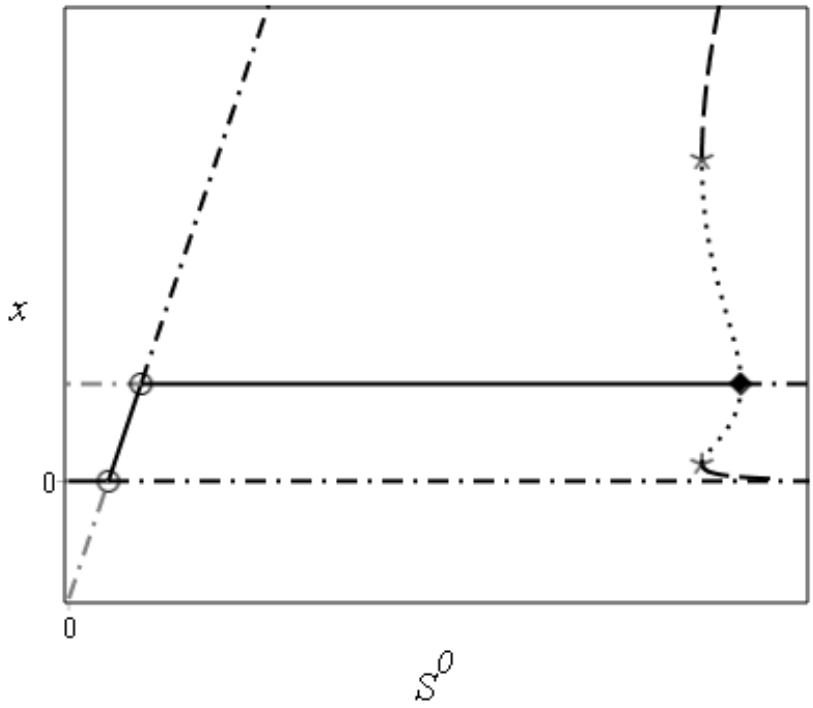

Figure 4.1: One-parameter bifurcation diagram of System (2.4) where $q = q_A$, $a = 2$, and $D = 0.5$. Solid lines and dash-dot lines represent stable and unstable equilibria, respectively. The dotted curves and long-dash curves represent unstable and stable limit cycles, respectively. A grey colouring indicates biologically irrelevant parameter space. These portions of the plot are still included to demonstrate the interchanging of stability. An open circle, filled diamond, and asterisk represent a transcritical bifurcation, subcritical Hopf bifurcation, and saddle node bifurcation of limit cycles, respectively.

Fix $a > 0$ and $D > 0$. Consider varying S^0. First we demonstrate that a transcritical bifurcation occurs at $S^0 = D$ where E_E and E_{ME} interchange stability. As this bifurcation does not involve E_I, we do not immediately concern ourselves with the relative ordering of parameters a and D. Assume S^0 is initially 0, but is increased so that $S^0 < D$ and $|S^0 - D|$ is arbitrarily small. Hence, E_{ME} is locally stable. Moreover, E_E and E_I do not exist in the first quadrant. However,

$$F'(K) = -\frac{K}{K + aq(K)}$$

where K is negative, but arbitrarily close to zero. Now $q'(0) > 0$ and q is continuous, hence, $q(K) < 0$. Therefore, $F'(K) > 0$ and so J_E has two negative terms on its main diagonal. J_E is upper triangular, hence, has two negative eigenvalues. Therefore, E_E is locally asymptotically stable for $S^0 < D$. If S^0 is increased further so that $S^0 = D$, then evidently E_{ME} and E_E temporarily coalesce. Assume S^0 is increased further still so that $S^0 > D$. Then both E_E and E_{ME} exist in the first quadrant. E_I, if it exists, is also in the first quadrant. In either case, $x^* > S^0 - D$, since $S^0 - D$ is arbitrarily small, but positive. In Section 2.3 it was already demonstrated that in this case E_E is locally asymptotically stable and E_{ME} is unstable. Hence, at $S^0 = D$ a transcritical bifurcation occurs where equilibria E_E and E_{ME} interchange stability.

Now we demonstrate that a transcritical bifurcation occurs when $S^0 = x^* + D$ where E_E and E_I interchange stability. Assume $a > D > 0$ so as to ensure the existence of E_I. If $S^0 - D$ is still an arbitrarily small, positive number, then $x^* > S^0 - D$. Consider increasing S^0 so that $S^0 - D$ is smaller than x^*, but only by an arbitrarily small amount. By Remark 2.2.2 $F'(K) < 0$, hence, since x^* and K are arbitrarily close together and F' is continuous, $F'(x^*) < 0$. Moreover, $F(x^*) < 0$, since $x^* > K$. Therefore, by equation (2.6), J_I has two real eigenvalues of opposing sign. Hence, E_I is

locally unstable. If we increase S^0 more so that $x^* = S^0 - D$, then E_E and E_I temporarily coalesce. If S^0 is increased yet again, so that $S^0 - D > x^*$, but $|S^0 - D - x^*|$ is arbitrarily small, then, as seen in Section 2.3, E_E is now unstable. Since $F'(K) < 0$, then $F'(x^*) < 0$. Moreover, $F(x^*)$ is positive, but arbitrarily close to zero. Hence, by equation (2.6), J_I has two negative real eigenvalues. Therefore, E_I is locally stable and so a transcritical bifurcation occurs at $S^0 = x^* + D$ where E_E and E_I interchange stability.

Next we demonstrate that System (2.4) undergoes a Hopf bifurcation when the interior equilibrium occurs at a local extremum of the prey nullcline. Let $\tilde{x}$ be a local maximum (respectively, minimum) value of the prey nullcline. By Theorem 3.3.1, the location of the extrema of the prey nullcline can be influenced by varying S^0. Assume S^0 is chosen so that $|x^* - \tilde{x}|$ is arbitrarily small. Further assume $x^* > \tilde{x}$ (respectively, $x^* < \tilde{x}$). Then $F'(x^*)$ is negative, but arbitrarily small. Hence, by equation (2.6), J_I has two complex eigenvalues with negative real part. As S^0 is increased, then, by Theorem 3.3.1, $\tilde{x}$ increases (respectively, decreases). Therefore, if we continue to increase S^0, eventually $\tilde{x}$ will equal x^* and $F'(x^*)$ will vanish. When $x^* = \tilde{x}$ equation (2.6) determines that J_I has two purely imaginary eigenvalues. As S^0 is increased so that $|x^* - \tilde{x}|$ is arbitrarily small while $x^* < \tilde{x}$ (respectively, $x^* > \tilde{x}$), then $F'(x^*)$ is positive and equation (2.6) determines that J_I has two eigenvalues with positive real parts. Hence, a Hopf bifurcation occurs when x^* coincides with a local extrema of the prey nullcline.

The existence of the Hopf bifurcation indicates the existence of periodic orbits in the phase-space of System (2.4). In Section 4.1 we consider the criticality of the Hopf bifurcation. If the Hopf bifurcation is subcritical, then there can exist an unstable periodic orbit surrounding an equilibrium point. Likewise, if the Hopf bifurcation is supercritical, then there can exist a stable periodic orbit surrounding an equilibrium point. We will first demonstrate two facts about the positioning of any periodic orbits.

Lemma 4.0.1. *Any periodic orbit of System (2.4) surrounds E_I.*

Proof. Any periodic orbit of the system must enclose one of the equilibria points. By Theorem 2.1.1, solutions remain non-negative. Hence, the periodic orbit cannot enclose either E_E or E_{ME} and so the lemma follows. □

Lemma 4.0.2. *Let Γ be any periodic orbit of System (2.4). Then*

$$\oint_\Gamma \operatorname{div}(\dot{x}, \dot{y})\,\mathrm{d}t = \oint_\Gamma (x + a\,q(x))F'(x)\,\mathrm{d}t$$

Proof.

$$\begin{aligned}
\oint_\Gamma \operatorname{div}(\dot{x}, \dot{y})\,\mathrm{d}t &= \oint_\Gamma [(a\,q(x) + x)F'(x) + \\
&\qquad (a\,q'(x) + 1)(F(x) - y) + a\,q(x) - D]\,\mathrm{d}t \\
&= \oint_\Gamma \left[(a\,q(x) + x)F'(x) + \frac{a\,q'(x) + 1}{a\,q(x) + x}\dot{x} + \frac{\dot{y}}{y}\right]\mathrm{d}t \\
&= \oint_\Gamma \left[(a\,q(x) + x)F'(x) + \frac{\mathrm{d}}{\mathrm{d}t}\ln(a\,q(x) + x) + \frac{\mathrm{d}}{\mathrm{d}t}\ln(y)\right]\mathrm{d}t \\
&= \oint_\Gamma (x + a\,q(x))F'(x)\,\mathrm{d}t
\end{aligned}$$

□

Theorem 4.0.1. *Any periodic orbit of System (2.4) surrounds a local extreme value of the prey-isocline $F(x)$.*

Proof. Let Γ be a periodic orbit of System (2.4). Suppose $F'(x)$ is of a single sign for all x along Γ. Suppose $F'(x) > 0$ (respectively, $F'(x) < 0$). Then, by Lemma 4.0.2, the contour integral of the divergence of the vector field along Γ is positive (respectively, negative). Hence, by the Poincaré criterion [4], Γ is an unstable (respectively, stable) periodic orbit. By Lemma 4.0.1 the periodic orbit surrounds E_I, hence, $F'(x^*) > 0$ (respectively, $F'(x^*) < 0$). Therefore, as seen in Section 2.3, E_I is unstable (respectively, stable). However, E_I and Γ cannot both simultaneously be unstable (respectively, stable). Therefore, $F'(x)$ cannot be of one sign along all of Γ. □

4.1 Criticality of the Hopf bifurcation

In this section we will demonstrate that in the case of an Ivlev or Monod response function the Hopf bifurcation is supercritical, but in the case of a Arctan or Hyperbolic Tangent response function the Hopf bifurcation can be super-critical or sub-critical, depending on if the extremum is a local minimum or a local maximum.

In Appendix D the vague-attractor condition Ω was derived. In particular, if $\Omega < 0$ then the Hopf bifurcation is supercritical and if $\Omega > 0$ then the Hopf bifurcation is subcritical. If $\Omega = 0$, then a Bautin bifurcation occurs at the equilibrium point.

$$\Omega \triangleq (x^* + D)F'''(x^*) - (x^* + D)F''(x^*)\frac{q''(x^*)}{q'(x^*)} + 2(aq'(x^*) + 1)F''(x^*)$$

As we have seen in Section 2.2 equation (2.5), when $S^0 = S^0(x^*)$, then the equilibrium point $(x^*, F(x^*))$ coincides with a local extremum of the prey nullcline.

Hence, we define

$$\hat{S}^0 \triangleq S^0(x^*) = (D + x^*)\frac{x^* + D - ax^*q'(x)}{D - ax^*q'(x^*)}. \tag{4.1}$$

Now, $\hat{S}^0$ is entirely determined by choice of (a, D). Furthermore, $x^* \triangleq q^{-1}\left(\frac{D}{a}\right)$, and as such x^* is also completely determined by choice of (a, D). Therefore, the vague-attractor condition of the Hopf bifurcation is a function entirely of (a, D).

It is a straightforward calculation to see that the vague-attractor condition at the Hopf bifurcation is

$$\begin{aligned}\hat{\Omega} \triangleq &\frac{(ax^{*2}q''(x^*) + 2D - 2ax^*q'(x^*))((D + x^*)q''(x^*) + aq'(x^*)^2 + q'(x^*))}{q'(x^*)(D + x^*)(D - ax^*q'(x^*))} \\ &- \frac{ax^{*2}q'(x^*)q'''(x^*)(D + x^*)}{q'(x^*)(D + x^*)(D - ax^*q'(x^*))}.\end{aligned} \tag{4.2}$$

Moreover, Theorem 4.1.1 will demonstrate the importance of the type of extremum the equilibrium point coincides with, so for convenience we also present here the second derivative of the prey nullcline at the equilibrium point

$$F''(x^*;\hat{S}^0) = -\frac{ax^{*2}q''(x^*) + 2d - 2ax^*q'(x^*)}{(D+x^*)(D-ax^*q'(x^*))}. \tag{4.3}$$

When an Ivlev or Monod response function is used in System (2.4), the prey nullcline can only have a local-maximum. However, when a Hyperbolic Tangent or Arctan response function is used, then the prey nullcline can have a local-maximum and a local-minimum. In this second case, the Hopf bifurcation can occur at either extremum. Consider using a Hyperbolic Tangent response function in System (2.4). In this situation we have many examples of the Hopf bifurcation occurring at the local minimum as a supercritical Hopf bifurcation (see $(a, D) = (7, 5)$) or a subcritical Hopf bifurcation (see $(a, D) = (7, 3)$). For the Arctan case take $(a, D) = (7, 3)$ and $(a, D) = (7, 1)$ for a supercritical and subcritical Hopf bifurcation, respectively. However, we have only observed a supercritical Hopf bifurcation at a local maximum, i.e. $(a, D) = (7, 6)$ for Hyperbolic Tangent and $(a, D) = (7, 5)$ for Arctan. This next theorem shows that at a local maximum, there can only be a supercritical Hopf bifurcation.

Theorem 4.1.1. *Assume either $q = q_A$ or $q = q_H$ and the Hopf bifurcation of System (2.4) occurs at a local maximum of the prey nullcline. The Hopf bifurcation is then supercritical. If the Hopf bifurcation of System (2.4) instead occurs at a local minimum of the prey nullcline, then the Hopf bifurcation can be supercritical or subcritical.*

Proof. Assume $q = q_A$ or $q = q_H$ and that the Hopf bifurcation of System (2.4) occurs at a local maximum of the prey nullcline. The proof proceeds in two parts. First, we demonstrate that $\hat{\Omega}$ increases as $F''(x^*;\hat{S}^0)$ increases. Secondly, we demonstrate that when $F''(x^*;\hat{S}^0) = 0$, the vague attractor

condition, $\hat{\Omega}$, is negative. Thus, in order for $\hat{\Omega}$ to be non-negative, $F''(x^*; \hat{S}^0)$ has to be positive. As a result, if $\hat{\Omega} > 0$, then $F''(x^*; \hat{S}^0) > 0$; from which the theorem follows.

By definition,

$$\hat{\Omega} \triangleq (x^* + D)F'''(x^*; \hat{S}^0) + \left(2(aq'(x^*) + 1) - (x^* + D)\frac{q''(x^*)}{q'(xs)}\right) F''(x^*; \hat{S}^0).$$

Since $q'(x^*) > 0$, $a > D > 0$, $x^* > 0$, and $q''(x^*) < 0$, the coefficient of $F''(x^*; \hat{S}^0)$ is positive. Hence, $\hat{\Omega}$ is an increasing function of $F''(x^*; \hat{S}^0)$.

We begin by taking $a > D > 0$, in order to ensure the existence of E_I. Since D, x^*, and $q(x) - xq'(x)$ are always positive (by Lemma 1.4.1), the denominator of $F''(x^*; \hat{S}^0)$ is always positive. Hence, $F''(x^*; \hat{S}^0) = 0$ if, and only if,

$$a{x^*}^2 q''(x^*) + 2D - 2ax^* q'(x^*) = 0. \tag{4.4}$$

Assume $F''(x^*; \hat{S}^0) = 0$. Then, as a consequence of Equation 4.4,

$$\hat{\Omega} = -\frac{a{x^*}^2 q'(x^*) q'''(x^*)(D + x^*)}{q'(x^*)(D + x^*)(D - ax^* q'(x^*))}.$$

Since $q'(x^*) > 0$ and $a > 0$, $\operatorname{sgn}(\hat{\Omega}) = -\operatorname{sgn}(q'''(x^*))$. We now focus on the two cases based on the choice of response function.

1. Let $q = q_H$. Then $q'''(x^*) = -2a^{-4}(a^2 - D^2)(a^2 - 3D^2)$. If $a < \sqrt{3}D$, then $\hat{\Omega} < 0$ and the lemma follows. All that is left to show is that $F''(x^*; \hat{S}^0) \neq 0$ for $a > \sqrt{3}D$.

   The numerator of $F''(x^*; \hat{S}^0)$ is $-a{x^*}^2 q''(x^*) + 2ax^* q'(x^*) - 2D$. Taking $q = q_H$ and $D = ua$ for some $0 < u < 3^{-1/2}$, then the numerator of $F''(x^*; \hat{S}^0)$ is

   $$p(u) \triangleq -2a(u(u^2 - 1)\operatorname{arctanh}(u)^2 + (u^2 - 1)\operatorname{arctanh}(u) + u).$$

Now, $p(0) = p'(0) = p''(0) = 0$ and $p'''(0) = 4a$. Hence, $p(u)$ is initially zero, but increasing. Moreover, $p'(u) = 2a(1 - 3u^2)\operatorname{arctanh}(u)^2$ which is positive for all $0 < u < 3^{-1/2}$.

The denominator of $F''(x^*; \hat{S}^0)$ is always positive and the numerator is positive for all $D < a < \sqrt{3}D$, hence, $F''(x^*; \hat{S}^0)$ is positive for all $D < a < \sqrt{3}D$, which is contrary to the initial supposition.

2. Assume $q = q_A$. Then

$$q'''(x^*) = \frac{4(3x^{*2} - 1)}{\pi(x^{*2} + 1)^3}$$

Hence, if $x^* > \frac{1}{\sqrt{3}}$, then the lemma follows. All that is left is to show that $F''(x^*; \hat{S}^0) \neq 0$ for $x^* < \frac{1}{\sqrt{3}}$. Assume $x^* < \frac{1}{\sqrt{3}}$. Then

$$\tan\left(\frac{\pi D}{2a}\right)^2 < \frac{1}{\sqrt{3}}$$

hence, $3D < a$. We proceed similarly as in the proof of the case where $q = q_H$. The numerator of $F''(x^*; \hat{S}^0)$ when $q = q_A$ and $D = ua$ for some $0 < u < 3^{-1}$ is $2\,a\,p(u)\tan\left(1/2\,u\pi\right)^{-2}\pi^{-1}$ where $p(u)$ is defined as

$$u - \pi\tan\left(\frac{u\pi}{2}\right)^4 + 4\tan\left(\frac{u\pi}{2}\right)^3 - 2u\pi\tan\left(\frac{u\pi}{2}\right)^2 + 2\tan\left(\frac{u\pi}{2}\right) - u\pi.$$

It is a straightforward calculation to see that $p(0) = p'(0) = p''(0) = 0$, but $p'''(u) = \frac{1}{2}\pi^3$. So $p(u)$ is initially zero and increasing. Consider

$$p'(u) = 2\pi\tan\left(\frac{u\pi}{2}\right)\left(\tan\left(\frac{u\pi}{2}\right)^2 + 1\right) r(u)$$

where

$$r(u) \triangleq -u\pi\tan\left(\frac{u\pi}{2}\right)^2 - u\pi + \frac{5}{2}\tan\left(\frac{u\pi}{2}\right).$$

Now $r(0) = 0$ and $r'(0) = 1/4\pi$. The second derivative of r is:

$$-\frac{\pi^2}{4}\left(1 + \tan\left(\frac{u\pi}{2}\right)^2\right)\left(6u\pi\tan\left(\frac{u\pi}{2}\right)^2 + 2u\pi + 3\tan\left(\frac{u\pi}{2}\right)\right).$$

Therefore, r is initially zero and initially increasing, but $r''(u) < 0$ for all $0 < u < 3^{-1}$. Hence, $p'(u)$ may change sign at most once. Since p is also initially zero and initially increasing, p may also change sign at most once. Now $0 < u < \frac{1}{3}$ and

$$p\left(\frac{1}{3}\right) = \frac{4}{27}\left(15\sqrt{3} - 8\pi\right) > \frac{4}{27}\left(15 \cdot 1.7 - 8 \cdot 3.15\right) = \frac{2}{45} > 0.$$

Hence, $p(u) > 0$ for all $0 < u < \frac{1}{3}$, and so the numerator of $F''(x^*; \hat{S}^0)$ is positive for all $D < a < 3D$.

The denominator of $F''(x^*; \hat{S}^0)$ is always positive, the numerator is positive for all $D < a < 3D$, hence, $F''(x^*; \hat{S}^0)$ is positive for all $D < a < 3D$, which is contrary to the initial supposition.

When $F''(x^*; \hat{S}^0) = 0$ we have $\hat{\Omega} < 0$ and as $F''(x^*; \hat{S}^0)$ increases so too does $\hat{\Omega}$. Hence, if $\hat{\Omega} > 0$, then $F''(x^*; \hat{S}^0) > 0$. Therefore, if $F''(x^*; \hat{S}^0) < 0$, then $\hat{\Omega} < 0$. This concludes the proof that any Hopf bifurcation of System (2.4) that occurs at a local maximum of the prey nullcline is necessarily supercritical.

To demonstrate the criticality of a Hopf bifurcation of System (2.4) that occurs at a local minimum of the prey nullcline, in the cases that $q \in \{q_A, q_H\}$, we provide parameter sets that yield appropriate values of $\hat{\Omega}$ and $F''(x^*; \hat{S}^0)$. In all of these examples, it is assumed that $S^0 = \hat{S}^0$ and so a and D are the only free parameters.

Assume $q = q_A$. For a supercritical Hopf bifurcation take $(a, D) = (7, 3)$. Note that, by (4.3), $F''(x^*; \hat{S}^0) = 0.0106\ldots > 0$ and, by (4.2), $\hat{\Omega} = -1.4202\ldots < 0$. Similarly, for a subcritical Hopf bifurcation take $(a, D) = (7, 3)$. Note that, by (4.3), $F''(x^*; \hat{S}^0) = 0.1998\ldots > 0$ and, by (4.2), $\hat{\Omega} = 2.0697\ldots > 0$.

Finally, assume $q = q_H$. For a supercritical Hopf bifurcation take $(a, D) = (7, 3)$. Note that, by (4.3), $F''(x^*; \hat{S}^0) = 0.0106\ldots > 0$ and, by (4.2), $\hat{\Omega} =$

$-1.4202\ldots < 0$. Similarly, for a subcritical Hopf bifurcation take $(a, D) = (7, 1)$. Note that, by (4.3), $F''(x^*; \hat{S}^0) = 0.7171\ldots > 0$ and, by (4.2), $\hat{\Omega} = 6.7492\ldots > 0$. □

Corollary 4.1.1. *Assume $q = q_M$ or $q = q_I$. The only Hopf bifurcation is supercritical.*

Proof. Let $q = q_M$ or $q = qI$, then by Theorem 3.1.1, there is only one local extrema of the prey isocline. Since $F'(0) > 0$ and $F(K) = 0$ for either $q = q_I$ or $q = q_M$, this local extrema corresponds to a local maximum. Supose $F''(x^*; \hat{S}^0) = 0$. Then, as seen in the proof of Theorem 4.1.1, $\operatorname{sgn}(\hat{\Omega}) = -\operatorname{sgn}(q'''(x^*))$.

1. Assume $q = q_M$. Then $q'''(x^*) = 6a^{-4}(a-d)^4 > 0$, hence, $\hat{\Omega} < 0$.

2. Assume $q = q_I$. Then $q'''(x^*) = a^{-1}(a-d) > 0$, hence, $\hat{\Omega} < 0$.

Therefore, as in the proof of Theorem 4.1.1, $\hat{\Omega}$ increases as $F''(x^*; \hat{S}^0)$ increases and if $F''(x^*; \hat{S}^0) = 0$, then $\hat{\Omega} < 0$. Hence, $\hat{\Omega} < 0$ for $F''(x^*; \hat{S}^0) < 0$. □

4.2 Two-Parameter Bifurcation Diagrams

In the following section we present two-parameter bifurcation diagrams. These diagrams were numerically calculated using `XPPAUT` [2] and plotted in Maple [1].

In Figure 4.2, the dotted line represents the transcritical bifurcation at $S^0 = D$, the dashed curve represents the transcritical bifurcation at $S^0 = D + x^*$, the solid curve represents the Hopf bifurcation, and the dash-dotted curve represents the saddle node bifurcation of limit cycles (cyclic fold bifurcation). The supercritical Hopf is the bold solid curve and the subcritical Hopf is the regular solid curve. The Bautin bifurcation (where the

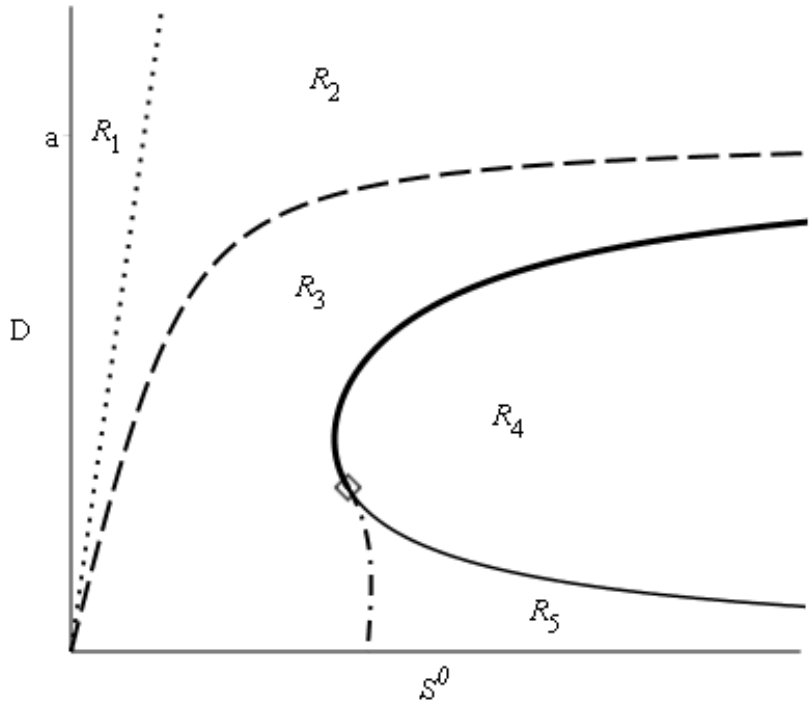

Figure 4.2: Two-parameter bifurcation diagram of System (2.4) with $q = q_A$. The diagram for $q = q_H$ is similar (See Figure 4.4). The dotted line is the transcritical bifurcation $S^0 = D$, the dashed curve is the transcritical bifurcation $S^0 = D + x^*$, the solid curve is the Hopf bifurcation given by $\hat{S}^0 = 0$, and the dash-dot curve is the saddle-node bifurcation of limit cycles.

supercritical and subcritical Hopf bifurcations meet) is labeled by a diamond. In particular, the diagram partitions the (S^0, D) space into five regions based on the number and type of equilibria. We now consider the dynamics of the system as we vary parameters throughout (S^0, D) space. In region R_1, only the mutual extinction equilibrium (E_{ME}) exists in the first quadrant. As we leave R_1 by passing over the transcritical bifurcation $S^0 = D$ into R_2 the prey-extinction equilibrium (E_E) enters the first quadrant. If we pass over the next transcritical bifurcation $S^0 = D + x^*$ into region R_3, the in-

terior, co-existence equilibrium (E_I) enters the first quadrant. Passing over the super-critical Hopf into R_4 a stable periodic orbit appears around E_I (Lemma 4.0.1) If we continue clockwise around the Bautin bifurcation, we enter into region R_5 by passing over the subcritical Hopf bifurcation and a new, unstable periodic orbit appears. Now multiple nested periodic orbits surround E_I (Lemma 4.0.1). Continuing clockwise pivoting around the Bautin bifurcation, we cross the saddle node bifurcation of limit cycles back into R_3 where the two stable and unstable periodic orbits annihilate. Typical examples of the phase-space for (S^0, D) in each region are presented in Figure 4.3.

In Figure 4.3 (a), we take $(S^0, D) \in R_1$ and so only the stable E_{ME} equilibrium exists in the first quadrant. In (b), we take $(S^0, D) \in R_2$ and so the stable E_E equilibrium now enters the first quadrant, moreover, equilibrium E_{ME} now becomes unstable. In (c), we take $(S^0, D) \in R_3$ where the stable E_I equilibrium exists in the first quadrant. The two extinction equilibria, E_E and E_{ME}, are now unstable. In (d), the predator nullcline x^* has moved to the left, past the local maximum of the prey nullcline, and a stable periodic orbit enters the first quadrant. In this case E_I, E_E, and E_{ME} are unstable. In (e), the predator nullcline x^* has moved left of the local minimum of the prey nullcline, an unstable periodic orbit is now nested inside the outer, stable, periodic orbit. The coexistence equilibrium E_I is now locally stable while the extinction equilibria, E_E and E_{ME}, remain unstable. These figures were generated with $(S^0, D, a) \in \{(1, 3, 1), (5, 3, 1), (10, 3, 3.001), (10, 3, 4), (10, 3, 19)\}$ and $q = q_H$.

4.3 Bifurcation Diagram Comparison

Assume we are modeling a biological system for some fixed S^0 and D. We have chosen our response functions $q(x)$ to be one of the four options

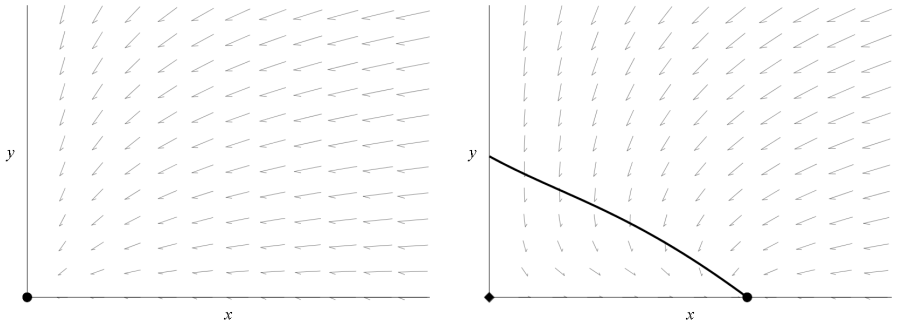

(a) $(S^0, D) \in R_1$ (b) $(S^0, D) \in R_2$

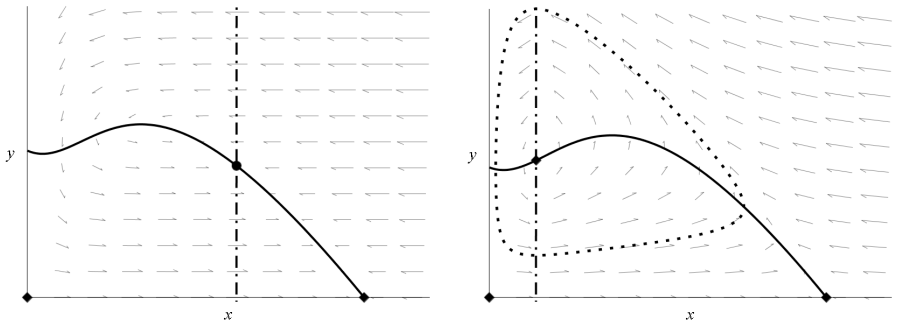

(c) $(S^0, D) \in R_3$ (d) $(S^0, D) \in R_4$

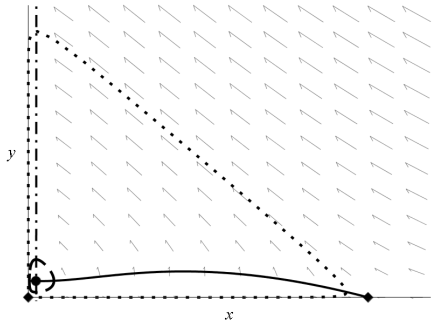

(e) $(S^0, D) \in R_5$

Figure 4.3: Phase space plots for various values of (S^0, D). The solid curve is the prey-nullcine $F(x)$, the dash-dot line is the predator nullcline x^*, and dashed and dotted curves are unstable and stable periodic orbits, respectively. Circles and diamonds mark stable and unstable equilibria, respectively.

q_M, q_I, q_A, q_H where the parameter a has been fit via least-squares methods, as previously. In this case we have four different models, we have already seen the qualitative differences in the phase-space between the models. For instance, the models parameterised by Monod or Ivlev response functions only attain one Hopf bifurcation (as a result of Theorem 3.1.1) where as those models parameterised by Hyperbolic Tangent or Arctan attain two Hopf bifurcations. Moreover, the second class of models can attain Hopf bifurcations of either criticality (as a result of Theorem 4.1.1) – and hence, a Bautin bifurcation – whereas the former class of models can only attain a supercritical Hopf bifurcation. Hence, we have partitioned our four models into two classes, based on the qualitative structure of their phase-space (moreover, this partitioning is entirely determined by Theorem 4.1.1 for these response functions). However, all four models produce quantitatively different results, as well.

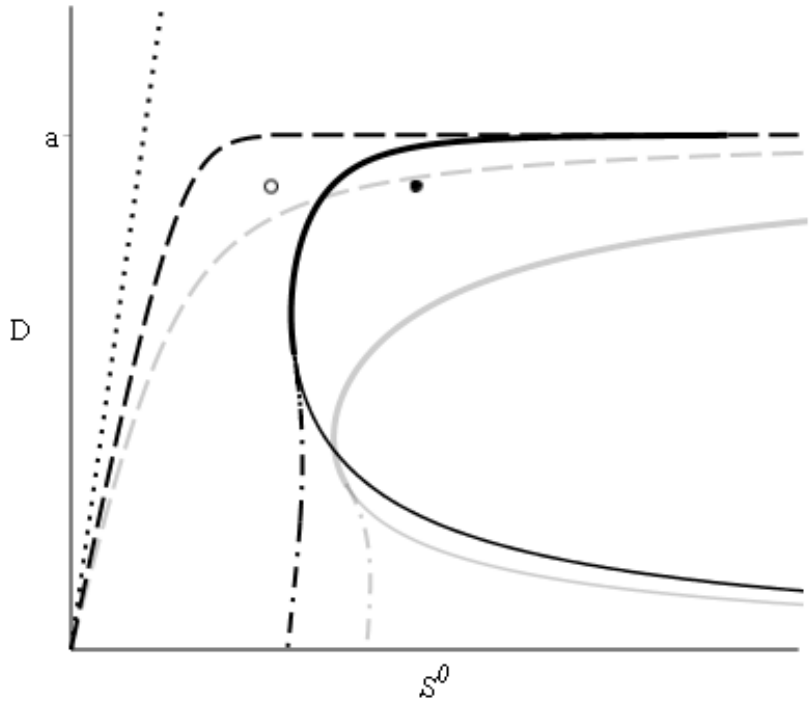

Figure 4.4: Two-parameter bifurcation diagram for Hyperbolic Tangent (black) overlaid by the two-parameter bifurcation diagram for Arctan (grey). Two points in (S^0, D) space are marked by empty and filled circles. The dotted line is the transcritical bifurcation $S^0 = D$, the dashed curve is the transcritical bifurcation $S^0 = D + x^*$, the solid curve is the Hopf bifurcation given by $\hat{S}^0 = 0$ from (4.1), and the dash-dot curve is the saddle-node bifurcation of limit cycles.

While S^0 and D are fixed for all four models, the parameter a differs depending on choice of response function. As a result, since x^* is implicitly a function of a, the transcritical bifurcation $S^0 = D + x^*$ and the Hopf bifurcation (occurring at $F'(x^*) = 0$) are quantitatively different among the four models. This is illustrated by the two points in Figure 4.4. The first point, marked by an empty circle, is in R_3 for Hyperbolic Tangent, but in

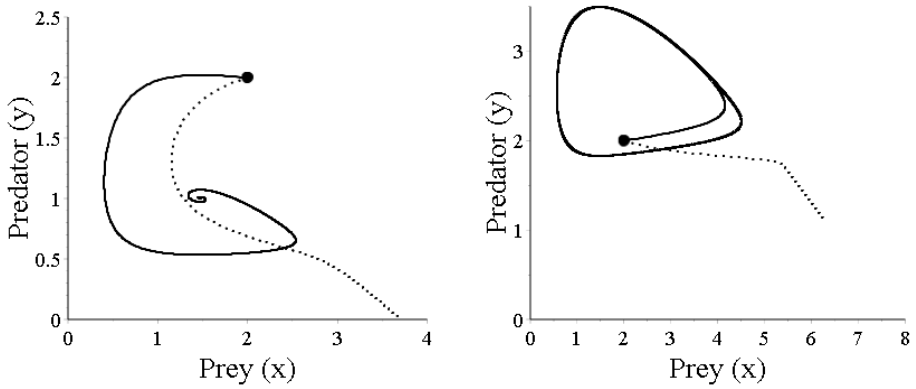

Figure 4.5: An example demonstrating trajectories for each of the two (S^0, D) pairs from Figure 4.4, $(S^0, D) = (5.5, 1.8)$ [left] and $(S^0, D) = (9.5, 1.8)$ [right], using the same initial conditions $x(0) = y(0) = 2$. The solid curve represents trajectories of the system with $q = q_H$ and the dotted curve trajectories of the system with $q = q_A$. The filled circle represents the starting point for each trajectory.

R_2 for Arctan. Similarly, the second point, marked by a filled circle, is in R_4 for Hyperbolic Tangent, but in R_3 for Arctan. The trajectories of these two points are illustrated in Figure 4.5, but the bifurcation analysis has already determined the result: for the first point, the Hyperbolic Tangent system predicts convergence to a coexistence equilibrium whereas the Arctan system predicts extinction of the predator and persistence of the prey; for the second point, the Hyperbolic Tangent system predicts convergence to a stable periodic orbit and the Arctan system predicts convergence to a coexistence equilibrium. Figure 4.4 and the analysis of the regions suggest other possible confounded predictions.

Suppose one wishes to model some predator-prey interaction. They gather data and find the predator-response function shape to be decidedly Holling Type II. The modeler may choose any two response functions that behave

comparably well under best least-squares fitting to the data. Given these conditions, for a large portion of (S^0, D) space the predictions of the different models that result could be qualitatively different depending on the exact functional form of the response function. As discussed previously, one model may predict coexistence of the predator and prey while another model might predict rapid extinction of the predator; it is impossible, by data collection and curve fitting alone, for the modeler to distinguish between either prediction with any confidence.

Chapter 5

Global Behaviour

The local dynamics of each equilibrium point have been determined in Section 2.3. Here we lay the groundwork for extending these results to claims about the global stability of the equilibria. We utilise a result of Harrison [5] to demonstrate that the interior equilibrium is globally asymptotically stable whenever a certain geometric condition of the location of E_I relative to the local extrema of the prey nullcline is met.

5.1 Globally Stable E_I

In [5] a generalised predator-prey system (5.1) is analysed (we have made the notational substitution $H = x$ and $P = y$ for convenience).

$$\begin{aligned} \dot{x} &= a(x) - f(x)b(y) \\ \dot{y} &= n(x)g(y) + c(y) \end{aligned} \tag{5.1}$$

The authors assume the existence of an equilibrium (x^*, y^*) interior to the first quadrant and propose the following Lyapunov function.

$$V(x,y) \triangleq \int_{x^*}^{x} \frac{n(r) - n(x^*)}{f(r)} \mathrm{d}r + \int_{y^*}^{y} \frac{b(r) - b(y^*)}{g(r)} \mathrm{d}r \tag{5.2}$$

Let

$$I_1 \triangleq \{x \in [0, S^0 - D] \,|\, F(x) > F(\tilde{x}) \text{ for all } \tilde{x} > x\}$$

and

$$I_2 \triangleq \{x \in [0, S^0 - D] \,|\, F(x) < F(\tilde{x}) \text{ for all } \tilde{x} < x\}.$$

We make a couple brief notes about the two sets. Immediately from the definition we see that if $\bar{x} \in (I_1 \cup I_2)$, then $F'(\bar{x}) < 0$. If $F'(0) > 0$ and F decreases somewhere on the interval $(0, S^0 - D)$, then F has a local maximum. Moreover, since F initially increases and $F'(K) < 0$ (Remark 2.2.2), there is a local maximum of F that is global on the interval $[0, S^0 - D]$. Hence, if $F'(0) > 0$, then $I_1 = \varnothing$. The set I_2, however, is always non-empty. Since, by Remark 2.2.2, $F'(S^0 - D) < 0$, $(S^0 - D) \in I_2$. Since F is continuous, I_2 contains some interval of $[0, S^0 - D]$. See Figure 5.1 for an illustration of I_1 and I_2 for the prey nullcline of System (2.4) with Arctan response function.

Theorem 5.1.1. *The interior equilibrium point E_I of System (2.4) is globally asymptotically stable if $x^* \in I_1 \cup I_2$*

Proof. First we note that System (2.4) is just a special case of System (5.1) under the following substitutions:

$$\begin{array}{lll} a(x) = F(x)(aq(x) + x) & f(x) = aq(x) + x & b(y) = y \\ n(x) = aq(x) - D & c(y) = 0 & g(y) = y \end{array}$$

Hence, for System (2.4), and equilibrium point E_I, the Lyapunov function from equation (5.2) becomes

$$\begin{aligned} V(x, y) &= \int_{x^*}^{x} \frac{a\,q(r) - D}{a\,q(r) + r} \mathrm{d}r + \int_{F(x^*)}^{y} \frac{r - F(x^*)}{r} \mathrm{d}r \\ &= \int_{x^*}^{x} \frac{a\,q(r) - D}{a\,q(r) + r} \mathrm{d}r + y - F(x^*) + F(x^*) \ln\left(\frac{F(x^*)}{y}\right) \end{aligned}$$

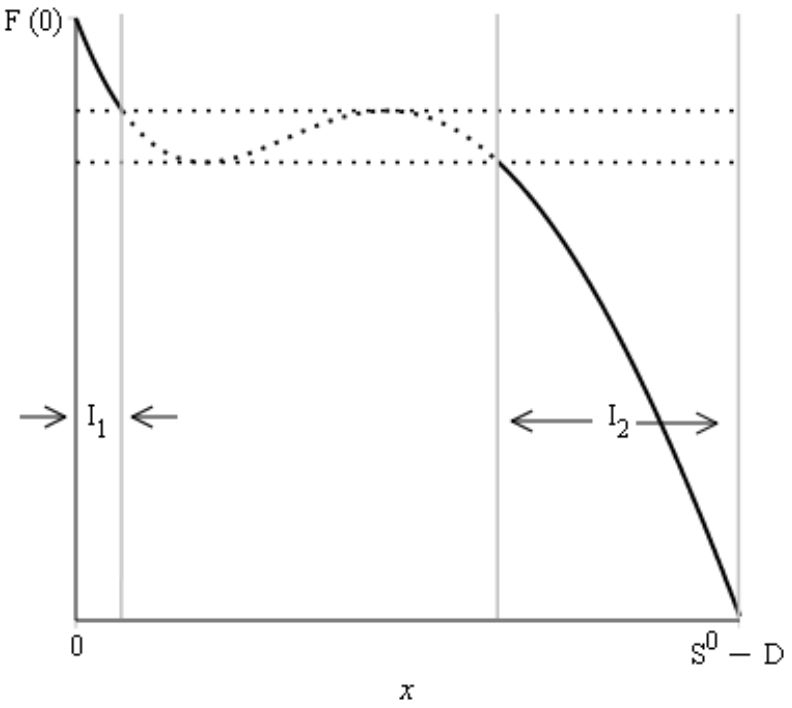

Figure 5.1: A plot demonstrating the x intervals I_1 and I_2.

Moreover, the trajectory derivative of V is

$$\begin{aligned}\dot{V}(x,y) &= \partial_x V\dot{x} + \partial_y V\dot{y} \\ &= \frac{aq(x)-D}{aq(x)+x}(F(x)-y)(aq(x)+x) + (y-F(x^*))(aq(x)-D) \\ &= (aq(x)-D)(F(x)-F(x^*)).\end{aligned}$$

By definition of I_1 and I_2, $F(x) - F(x^*)$ is negative for all $x > x^*$ and positive for all $x < x^*$. Since $q(x)$ is increasing for all $x > 0$ and $aq(x^*) = D$ we also have that $a\,q(x) - D$ is positive for all $x > x^*$ and negative for all $x < x^*$. Hence, $\dot{V}(x,y) \leq 0$ for all (x,y) in the first quadrant with equality if, and only if, $x = x^*$. Hence, by LaSalle's invariance principle (see, for example

[8]), all bounded trajectories converge to the largest invariant subset of

$$\{(x, y) \,|\, x = x^* \text{ and } y \geq 0\} = \{(x^*, F(x^*))\}.$$

Therefore, E_I is globally asymptotically stable and the theorem follows. □

If the predator nullcline is positioned high enough up on the initial downslope (or far enough down on the final downslope) of the prey nullcline, then the equilibrium is a global attractor. In Chapter 4, it was observed that a saddle node of limit cycles occurs where the predator nullcline is on the initial downslope of $F(x)$. In this case two nested limit cycles can appear (see, for instance, Figure 4.3 (e)). Therefore, the restriction of x^* to this small portion of the initial downslope seems justified. Figure 4.3 (e) gives an example of a stable E_I that is not globally asymptotically stable. Note that restricting x^* to $I_1 \cup I_2$ is not a necessary condition, there are examples of x^* far enough down the initial down slope that appear to be globally asymptotically stable. The following corollary covers the corner case where $F(x)$ is always non-increasing.

Corollary 5.1.1. *Assume $F(x)$ is always non-increasing and there is at most one point, $\bar{x}$, where $F'(\bar{x}) = 0$. Further, assume E_I exists in the interior of the first quadrant. Then, E_I is globally asymptotically stable.*

Proof. If $F(x)$ is always decreasing then $I_1 = I_2 = [0, S^0 - D]$ and the corollary follows immediately from Theorem 5.1.1. Assume there exists a point $\bar{x}$ where $F'(\bar{x}) = 0$. Then, $I_1 \cup I_2 = [0, \bar{x}) \cup (\bar{x}, I_2]$. If $x^* \in (I_1 \cup I_2)$, then the corollary follows immediately from Theorem 5.1.1. Assume $x^* \notin (I_1 \cup I_2)$. Then $x^* = \bar{x}$. The trajectory derivative of V is still $\dot{V}(x, y) = (a\, q(x) - D)(F(x) - F(x^*)) \leq 0$ with equality if, and only if, $x = x^* = \bar{x}$. Hence, the proof proceeds identically as in Theorem 5.1.1 and the corollary follows. □

Notice that both Theorem 5.1.1 and Corollary 5.1.1 give conditions for when the equilibrium $E_I = (x^*, y^*)$ in System (2.4) is globally asymptotically stable. Assume E_I is globally asymptotically stable. By Theorem A.1, the equilibrium $(S^0 - x^* - y^*, x^*, y^*)$ in System (1.2) is also globally asymptotically stable.

Consider the two predator response functions q_A and q_H. When x^* is positioned far enough down the initial downslope of $F(x)$ or when x^* is on a portion of $F(x)$ where F is increasing, then there is no hope of proving global asymptotic stability as we have already demonstrated the existence of periodic orbits for certain parameter sets in these cases. It is natural to ask what happens if x^* is positioned high-enough up on the final downslope of F. In Chapter 4 no saddle node bifurcation of limit cycles was observed for x^* in that region of the prey nullcline. In fact, there are examples where x^* in that region appears to be globally asymptotically stable.

In [12], the authors use an argument based on the Dulac criterion to demonstrate that in a Rosenzweig-MacArthur predator-prey system where the isocline takes on a similar shape to $F(x)$ (when parameterised by q_A or q_H), that their interior equilibrium is globally asymptotically stable for the entire final downslope of the prey nullcline. We conjecture that this is also true in System (2.4), but leave it as a future avenue of discovery.

Chapter 6

Conclusions and Future Work

We analysed a system of ODEs modeling predator-prey interactions in a chemostat. We demonstrated the sensitivity of this model to the choice of predator response function – even when these predator response functions have the same qualitative shape. In particular, it was shown that while the corresponding systems undergo the same transcritical bifurcations for these Holling Type II response functions, the systems can obtain differing numbers of Hopf bifurcations. When a Monod response function is used in System (2.4), a unique periodic orbit is observed (see [6]). In this thesis examples were given where Hyperbolic Tangent or Arctan response functions can instead result in non-uniqueness of the periodic orbit, i.e. two coexisting periodic orbits.

Biological relevance of solutions of systems (1.2) and (2.4) was determined by demonstrating that solutions of the system with positive initial conditions remain positive and bounded for all positive time. Moreover, we demonstrated that the original three dimensional system (1.1) is asymptotically equivalent to the limiting two dimensional system (2.4) with fewer parameters. We derived the three equilibrium points of System (2.4) corresponding to mutual extinction, predator extinction, and predator-prey coexistence.

We analysed the local stability of each of these equilibria points. A parameter free condition to determine the number of local extrema of the prey nullcline was derived. This is particularly useful as we demonstrated that a Hopf bifurcation always occurs at a local extremum of this prey nullcline. In particular, we show that Hyperbolic Tangent or Arctan response functions result in a prey-nullcline with a local maximum and a local minimum, while Monod and Ivlev response functions result in a prey-nullcline with only a local maximum. We demonstrated that a Hopf bifurcation occurring at a local minimum of the prey-nullcline can be either supercritical or subcritical in the case of Hyperbolic Tangent or Arctan response functions. Moreover, for these systems a Bautin bifurcation can occur. If the Hopf bifurcation occurs at a local maximum of the prey-nullcline for System (2.4) with Hyperbolic Tangent, Arctan, Monod, or Ivlev response functions, then the Hopf bifurcation is always supercritical. The dependence of these extrema on parameters was investigated and it was demonstrated that as S^0 increases, local maxima move up and to the right while local minima move up and to the left. Another parameter free condition was presented that demonstrates that System (2.4) for Arctan, Hyperbolic Tangent, or Ivlev response function has a prey nullcline with at most one inflection point. The prey nullcline of system (2.4) for the Monod response function was directly shown to have no inflection points.

We were able to demonstrate the global stability of the coexistence equilibrium for a section of parameter space and provide motivation to extend this result. Moreover, a bifurcation theory approach led to characterising the number of periodic orbits under various partitions of parameter space, but the exact number of coexisting periodic orbits was not analytically demonstrated. However, we conjecture that System (2.4) with Arctan or Hyperbolic Tangent response function can have at most two periodic orbits.

The two dimensional system (2.4) is just the three dimensional system

(1.2) evaluated on the simplex $s + x + y = S^0$. Trajectories of System (1.2) converge exponentially to the simplex. We demonstrated that globally stable equilibria in the two dimensional system (2.4) have corresponding global equilibria on the simplex in the three dimensional system (1.2). Hence, the results determining the criticality of the Hopf bifurcation, the local stability of equilibria, and the number of periodic orbits all have equivalent results on the simplex $s + x + y = S^0$ in the three dimensional system (1.2).

Analysis of the four response functions considered suggests topological equivalence of models based on the number of extrema, as determined by the parameter-free condition of Theorem 3.1.1. It would be interesting to see if this equivalence could be rigorously shown to be true, either in the case of the chemostat predator-prey system considered here or the Rosenzweig-MacArthur predator-prey system considered elsewhere (see [11, 13] for instance).

It was also observed, by way of bifurcation theory, that differing numbers of local extrema in the prey nullcline lead to differing sets of possible qualitative dynamics. However, even in the case of two response functions that produce the same number of local extrema in the prey nullcline, by overlaying two-parameter bifurcation diagrams one can see that the same choice of parameters and initial conditions can produce qualitatively different individual predictions (see Figure 4.4). This should be a real warning for modelers. By least-squares curve fitting the two functions may look entirely the same, and fit experimental data just as well, but for particular nutrient saturations (S^0) and flow-rates (D) the model with one response function may predict coexistence of predator and prey while another may predict rapid extinction of the predator.

Under Theorem 3.1.1 it is demonstrated that the Monod and Ivlev response functions can have at most one local extremum in the prey nullcline and Hyperbolic Tangent and Arctan can have at most two local extrema

in the prey nullcline. It is natural to ask how many total roots the $H(x)$ condition from Theorem 3.1.1 can have for Holling Type II $q(x)$ satisfying Definition 1.4.1. We conclude with the following intriguing, though admittedly not the most biologically relevant, example.

Example 6.0.1. Consider $q_3(x) \triangleq q_M(x) + 2q_H(x)$. Then, as demonstrated in Figure 6.1, the $H(x)$ condition from Theorem 3.1.1 has two roots. Hence, $F(x)$ parameterised by $q = q_3$ can have at most three local extrema (see Figure 6.2).

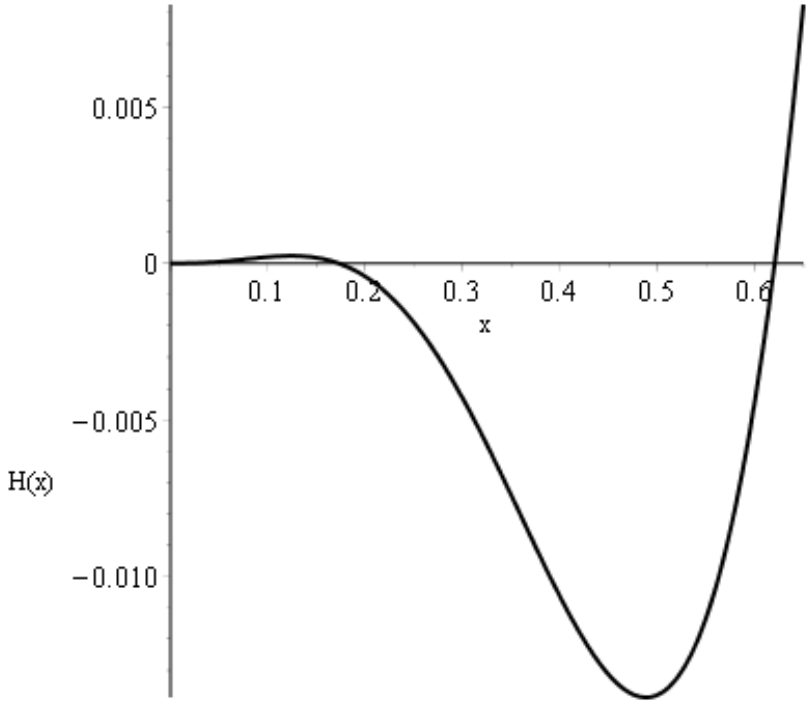

Figure 6.1: A plot of $H(x)$ with $q(x) = q_3(x) \triangleq q_M(x) + 2q_H(x)$. The plot illustrates that $H(x)$ has two positive roots, hence, the prey isocline under q_3 has at most three local extrema.

Let x_1 and x_2 be the two positive roots of $H(x)$ under q_3 (numerically, $x_1 = 0.1724313\ldots$ and $x_2 = 0.6204676\ldots$). Then $\hat{K}(x_1)$ is a critical point

of $\hat{K}$. Hence, for any value between $\hat{K}(x_1)$ and $\hat{K}(x_2)$ a horizontal line will have the maximum number of intersections with the $\hat{K}(x)$ curve (three, in this case). Hence, we define $K_3 \triangleq \frac{1}{2}\left(\hat{K}(x_1) + \hat{K}(x_2)\right)$. Consider the plot of $F(x; K_3)$ with $q = q_3$, as shown in Figure 6.2. The prey nullcline has three local extrema, hence, the system can undergo three different Hopf bifurcations (by (2.6)).

This raises a natural question, is there an upper limit on the possible number of roots of $H(x)$ for a response function $q(x)$ satisfying Definition 1.4.1?

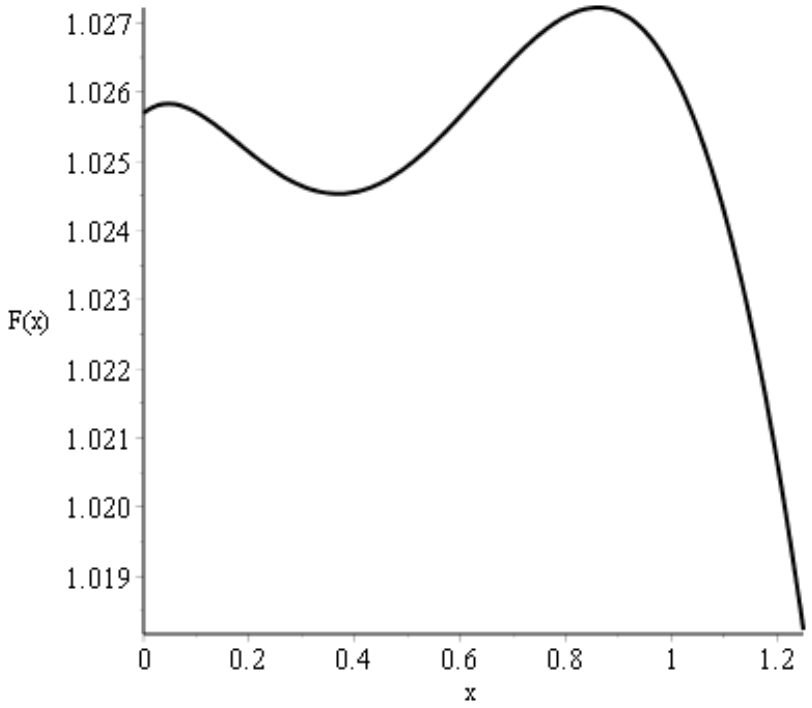

Figure 6.2: A plot of the prey nullcline of $F(x; K_3)$ where $q = q_3$, as predicted by Figure 6.1, the prey nullcline exhibits three local extrema. In this plot $a = 0.8$ and $K = S^0 - D = K_3 \approx 4.35875306$.

Appendix A

Smith and Waltman Convergence Theorem

A theorem from [14] is used to demonstrate that a globally attractive equilibrium (x^*, y^*) interior to the first quadrant of the limiting system (2.4) is a globally attractive equilibrium $(S^0 - x^* - y^*, x^*, y^*)$ in the first octant of the original system (1.2)

Theorem A.1. *(Smith and Waltman, 1995, [14]) Consider the two systems of ODEs of the form*

$$z' = Az, \qquad y' = f(y, z), \tag{A.1}$$

and

$$x' = f(x, 0) \tag{A.2}$$

where $z \in \mathbb{R}^m$, $(y, z) \in \mathcal{D} \subset (\mathbb{R}^n \times \mathbb{R}^m)$, *and* $x \in \Omega = \{x : (x, 0) \in \mathcal{D}\} \subset \mathbb{R}^n$. *Assume that* $\mathcal{D}$ *is positively invariant for (A.1), and (A.1) is dissipative. Let* $(y(t), z(t))$ *be a solution of (A.1), and assume the following hypotheses are satisfied:*

1. *All of the eigenvalues of A have negative real parts*

2. *Equation (A.2) has a finite number of equilibria in Ω, each of which is hyperbolic for (A.1). Denote these equilibria by $E_1, \ldots, E_p$.*

3. *The dimension of the stable manifold of E_i, denoted $M^+(E_i)$, is n for $1 \leq i \leq r$, and the dimension of the stable manifold of E_j is less than n for $(r+1) \leq j \leq p$.*

4. $\Omega = \cup_{i=1}^{p} M^+(E_i)$.

5. *Equation (A.2) does not possess a cycle of equilibria.*

Then, for some i, $\lim_{t\to\infty}(y(t), z(t)) = (E_i, 0)$.

Proof. Assume $E_I = (x^*, y^*)$ in System (2.4) exists in the interior of the first quadrant. Further, assume E_I is a globally asymptotically stable equilibrium point. We demonstrate that $(S^0 - x^* - y^*, x^*, y^*)$ is a globally asymptotically stable equilibrium point in System (1.2).

Let $z = S^0 - (s + x + y)$. Then, System (1.2) is then just a special case of System (A.1):

$$\begin{aligned} \dot{z} &= -Dz \\ \dot{x} &= (-D + S^0 - z - x - y)x - a\,y\,q(x) \\ \dot{y} &= y\,(a\,q(x) - D) \end{aligned} \tag{A.3}$$
$$z(0) \leq S^0, x(0) \geq 0, y(0) \geq 0.$$

A closed form for z can immediately be obtained, demonstrating that System (A.3) is dissipative and when $z = 0$ trajectories satisfy System 2.4.

In the notation of the theorem statement from [14], $n = 2$ and $m = 1$. Hence, 1. is trivially satisfied as A is the 1×1 matrix $[-D]$ with $D > 0$ (and so has one real, strictly negative eigenvalue).

System 2.4 has three equilibria. For notational ease, define $E_1, E_2, E_3 = E_I, E_E, E_{ME}$, respectively. In Section 2.3 it was demonstrated that when E_I

exists in the interior of the first quadrant all equilibria are hyperbolic, hence, 2. is satisfied.

Equilibrium E_1 is a global attractor for System (2.4), so the dimension of its stable manifold is $2 = n$. The other two equilibria, E_2 and E_3, are locally unstable saddles, hence, the dimension of their stable manifolds are both $1 < n = 2$. Therefore, 3. is satisfied.

Hypothesis 4. is satisfied, since any trajectories on Ω converge to one of the three equilibria E_1, E_2, E_3.

Finally, the stable manifold of E_2 is the line $\{(x, y) \,|\, y = 0 \text{ and } x \geq 0\}$. Moreover, the stable manifold of E_3 is the line $\{(x, y) \,|\, y \geq 0 \text{ and } x = 0\}$. Hence, E_2 and E_3 cannot form a chain of equilibria. Since E_1 is locally asymptotically stable, it also is not a part of any chain of equilibria. Hence, 5. is satisfied. □

Appendix B

Counting Prey Nullcline Extrema

This appendix contains the proofs of the Corollaries from Section 3.1. In particular, these corollaries use Theorem 3.1.1 to determine the number of local extrema the prey nullcline exhibits under various predator response functions (Monod, Ivlev, and Hyperbolic Tangent are all shown here, a proof for Arctan is presented in Section 3.1). Equation (3.2) is repeated here for convenience.

$$H(x) \triangleq x^2 q''(x) + 2(q(x) - xq'(x))$$

Corollary B.1. *The prey nullcline (2.3) with Monod response function has at most one local extremum.*

Proof. Let $q = q_M$. Taking $H(x)$ as defined in (3.2) gives

$$H(x) = \frac{2x^3}{(1+x)^3}.$$

Recognising $H(0) = 0$. Now $H'(x) = \frac{6x^2}{(x+1)^4} > 0$ hence, by Theorem 3.1.1, the corollary follows. □

Corollary B.2. *The prey nullcline (2.3) with Ivlev response function has at most one local extremum.*

Proof. Let $q = q_I$. Taking $H(x)$ as defined in (3.2) gives

$$H(x) = 2 - e^{-x}\left(x^2 + 2x + 2\right).$$

Again we can see that $H(0) = 0$. Now $H'(x) = x^2\mathrm{e}^{-x} > 0$. Hence, by Theorem 3.1.1, the corollary follows. □

Corollary B.3. *The prey nullcline (2.3) with Hyperbolic Tangent response function has at most two local extrema.*

Proof. Let $q = q_H$. Taking $H(x)$ as defined in (3.2) gives

$$H(x) = 2x^2\tanh(x)^3 + 2x\tanh(x)^2 + 2(1 - x^2)\tanh(x) - 2x.$$

As in the proof of Corollary 3.1.1 we see that $H'(0) = H''(0) = 0$ and $H'''(0) = -2 < 0$. Now,

$$H'(x) = -2x^2\left(3\tanh(x)^4 - 4\tanh(x)^2 + 1\right)$$

which has one positive root at $\operatorname{arctanh}\left(\frac{1}{\sqrt{3}}\right)$ (since the second factor in $H'(x)$ is quadratic in $\tanh(x)^2$). Furthermore $H(x)$ is eventually positive, since

$$\begin{aligned} H(\ln(9)) &= \frac{134480 - 13284\ln(3) - 25920\ln(3)^2}{68921} \\ &> \frac{56720 - 13284\sqrt{3}}{68921} \quad (\text{Since } \ln(x) < \sqrt{x}) \\ &> \frac{30152}{68921} \quad (\text{Since } \sqrt{3} < 2) \end{aligned}$$

Hence, $H(x)$ initially decreases, has at most one extremum for positive x, and is eventually positive for positive x. Therefore, $H(x)$ has exactly one positive root, and so by Theorem 3.1.1 the corollary follows. □

Appendix C

Counting Prey Nullcline Inflection Points

This appendix contains proofs for the number of inflection points that the prey nullcline has when parameterised by Ivlev and Hyperbolic Tangent response functions. Proofs for when the prey nullcline is parameterised by Monod and Arctan response functions were given in Section 3.2.

The definition of $\eta(x)$ is repeated here for convenience.

$$\eta(x) \triangleq x(q(x) - xq'(x))q'''(x) + \frac{3}{2}q''(x)(2(q(x) - xq'(x)) + x^2q''(x)).$$

Theorem C.1.

i. $F(x)$ *parameterised by* $q(x) = q_I(x)$ *has at most one inflection point*

iii. $F(x)$ *parameterised by* $q(x) = q_H(x)$ *has at most one inflection point*

Proof. i. $\eta(x) = \frac{1}{2}e^{-x}p(x)$ where $p(x) \triangleq (x^2 + 4x + 6)e^{-x} + 2x - 6)$. Since $e^{-x} > 0$, $\eta(x) = 0$ if, and only if, $p(x) = 0$. It is straightforward to check that $p(0) = p'(0) = 0$. Furthermore, $p''(x) = x^2e^{-x} > 0$, hence, $p(x) > 0$ for all $x > 0$. So, by Lemma 3.2.1, the theorem follows.

iii. In the case of $q(x) = q_H(x)$,

$$\eta(x) = \frac{2p(x)(\tanh(x)+1)(1-\tanh(x))}{e^{4x}+2e^{2x}+1}$$

where $p(x) \triangleq 2xe^{4x}-3e^{4x}+4x^2e^{2x}+6e^{2x}-2x-3$. Hence, $\eta(x) = 0$ if, and only if, $p(x) = 0$. Now $p(0) = p'(0) = 0$ and $p''(x) = 16e^{2x}(x^2+2x+2+2e^{2x}(x-1))$. So $p''(x)$ is positive if, and only if, that second factor

$$h(x) \triangleq x^2 + 2x + 2 + 2e^{2x}(x-1)$$

is positive. Similarly, we see that $h(0) = h'(0) = 0$. Hence, $\eta(x) > 0$ if, and only if, $h''(x) > 0$. Furthermore, $h''(x) = 8xe^{2x} + 2$ which is evidently positive for all $x > 0$. Hence, by Lemma 3.2.1, the theorem follows. □

Appendix D

Deriving the Vague Attractor Condition

In this appendix we derive the "vague attractor condition" Ω. In particular, if $\omega < 0$, then the Hopf bifurcation is supercritical and if $\omega > 0$, then the Hopf bifurcation is subcritical. This lengthy calculation follows the formula of [10] and results in a vague attractor condition identical to that derived in [13] for a similar predator-prey model.

Lemma D.1. *Let A be a matrix with complex eigenvalues $\alpha \pm i\beta$ with corresponding eigenvectors $P_{\Re} \pm iP_{\Im}$. Then $P = [P_{\Re} \mid P_{\Im}]$ is an invertible matrix with*

$$P^{-1}AP = \begin{bmatrix} \alpha & \beta \\ -\beta & \alpha \end{bmatrix}$$

Proof. Assume A and P are defined as in the lemma statement. Then

$$I = P^{-1}P = [P^{-1}P_{\Re} \mid P^{-1}P_{\Im}].$$

Hence, $P^{-1}P_{\Re} = [1, 0]^T$ and $P^{-1}P_{\Im} = [0, 1]^T$. Furthermore, $A(P_{\Re} + iP_{\Im}) = (\alpha + i\beta)(P_{\Re} + iP_{\Im})$, hence, by collecting real and imaginary parts of either

side: $AP_{\Re} = \alpha P_{\Re} - \beta P_{\Im}$ and $AP_{\Im} = \beta P_{\Re} + \alpha P_{\Im}$. Hence,

$$\begin{aligned} P^{-1}AP &= [P^{-1}AP_{\Re} \mid P^{-1}AP_{\Im}] \\ &= [P^{-1}(\alpha P_{\Re} - \beta P_{\Im}) \mid P^{-1}(\beta P_{\Re} + \alpha P_{\Im})] \\ &= \left[\alpha \begin{bmatrix} 1 \\ 0 \end{bmatrix} - \beta \begin{bmatrix} 0 \\ 1 \end{bmatrix} \;\middle|\; \beta \begin{bmatrix} 1 \\ 0 \end{bmatrix} + \alpha \begin{bmatrix} 0 \\ 1 \end{bmatrix} \right] \\ &= \begin{bmatrix} \alpha & \beta \\ -\beta & \alpha \end{bmatrix} \end{aligned}$$

□

Let S^0 be in a neighbourhood of $\hat{S}^0$, then $F'(x^*)$ is sufficiently smaller in magnitude than the positive quantity $4aF(x^*)q'(x^*)/(D + x^*)$. By equation (2.6), the eigenvalues of the Jacobian Matrix J_I corresponding to the coexistence equilibrium E_I for S^0 in such a neighbourhood are

$$\lambda_{I_{+,-}} = \frac{D + x^*}{2} \left(F'(x^*) \pm i \sqrt{\frac{4aF(x^*)q'(x^*)}{D + x^*} - F'(x^*)^2} \right)$$

with corresponding eigenvectors

$$V_{I_{+,-}} = \begin{bmatrix} D + x^* \\ \lambda_{I_{-,+}} \end{bmatrix}.$$

Hence, by Lemma D.1, the similarity transform P can be constructed by taking real and imaginary parts of the eigenvector corresponding to λ_{I_+}. This allows us to linearise System (2.4) so that the linear part is in real Jordan canonical form:

$$\begin{aligned} \begin{bmatrix} \dot{x} \\ \dot{y} \end{bmatrix} &= J_I \begin{bmatrix} x \\ y \end{bmatrix} + N_L \\ &= P \begin{bmatrix} \alpha & \beta \\ -\beta & \alpha \end{bmatrix} P^{-1} \begin{bmatrix} x \\ y \end{bmatrix} + N_L \\ P^{-1} \begin{bmatrix} \dot{x} \\ \dot{y} \end{bmatrix} &= \begin{bmatrix} \alpha & \beta \\ -\beta & \alpha \end{bmatrix} P^{-1} \begin{bmatrix} x \\ y \end{bmatrix} + P^{-1}N_L \end{aligned}$$

where

$$\alpha = \frac{F'(x^*)(D+x^*)}{2}, \quad \beta = \frac{D+x^*}{2}\sqrt{\frac{4a\,F(x^*)\,q'(x^*)}{D+x^*} - F'(x^*)^2},$$

(the real and imaginary parts of λ_{I_+}), N_L is the collection of non-linear (super-linear) terms, and the transition matrix

$$P = \left[\begin{array}{c|c} D+x^* & 0 \\ \alpha & -\beta \end{array}\right].$$

Under the change of variables $[u \mid v]^T = P^{-1}[x \mid y]^T$ the linearisation of System (2.4) becomes

$$\begin{bmatrix} \dot{u} \\ \dot{v} \end{bmatrix} = \begin{bmatrix} \alpha & \beta \\ -\beta & \alpha \end{bmatrix} \begin{bmatrix} u \\ v \end{bmatrix}.$$

Under the same change of variables the vector field from System (2.4) becomes

$$\begin{aligned} \dot{x}\big|_{[x|y]^T=P[u|v]^T} &= (F(u\,(D+x^*)) - \alpha u + \beta v)\cdot \\ &\qquad (a\,q(u\,(D+x^*)) + (D+x^*)u) \triangleq f(u,v) \\ \dot{y}\big|_{[x|y]^T=P[u|v]^T} &= (\alpha u - \beta v)\,(a\,q(u\,(D+x^*)) - D) \triangleq g(u,v) \end{aligned}$$

Therefore, by [10] Formula 4.2 the vague attractor condition can be computed as

$$\begin{aligned} W''' \triangleq\ & \frac{3\pi}{4|\beta|}\left(\partial^3_{uuu}f + \partial^3_{uvv}f + \partial^3_{uuv}g + \partial^3_{vvv}g\right) \\ & + \frac{3\pi}{4|\beta|^2}\left(-\partial^2_{uv}f\left(\partial^2_{uu}f + \partial^2_{vv}f\right) + \partial^2_{uv}g\left(\partial^2_{uu}g + \partial^2_{vv}g\right)\right) \\ & + \frac{3\pi}{4|\beta|^2}\left(\partial^2_{uu}f\partial^2_{uu}g - \partial^2_{vv}f\,\partial^2_{vv}g\right). \end{aligned}$$

evaluated at $[u|v]^T = P^{-1}[x^*|F(x^*)]$.

This calculation yields $W''' = \frac{3\pi}{4|\beta|}\frac{x^*+D}{aF(x^*)q'(x^*)}\Omega$ where

$$\Omega \triangleq (x^*+D)F'''(x^*) - (x^*+D)F''(x^*)\frac{q''(x^*)}{q'(x^*)} + 2(aq'(x^*)+1)F''(x^*)$$

which agrees with (up to a change in notation) the quantity derived in Wolkowicz [13] under a similar system to System (2.4).

Bibliography

[1] Maple 2015. *Maplesoft, a division of Waterloo Maple Inc.* Waterloo, Ontario.

[2] Bard Ermentrout. *Simulating, analyzing, and animating dynamical systems: a guide to XPPAUT for researchers and students.* SIAM, 2002.

[3] Gregor F Fussmann and Bernd Blasius. Community response to enrichment is highly sensitive to model structure. *Biology Letters*, 1(1):9–12, 2005.

[4] Jack K. Hale. *Ordinary Differential Equations.* Wiley-Interscience, 1969.

[5] Gary W. Harrison. Global stability of predator-prey interactions. *Journal of Mathematical Biology*, 8(2):159–171, Sep 1979.

[6] Madeleine Hill. A predator-prey model in the chemostat with Holling type II dynamics. *Masters Project, McMaster University*, 2016.

[7] Crawford S Holling. The components of predation as revealed by a study of small-mammal predation of the european pine sawfly. *The Canadian Entomologist*, 91(5):293–320, 1959.

[8] J LaSalle. Some extensions of Liapunov's second method. *IRE Transactions on circuit theory*, 7(4):520–527, 1960.

[9] Alfred J Lotka. Undamped oscillations derived from the law of mass action. *Journal of the American Chemical Society*, 42(8):1595–1599, 1920.

[10] Jerrold E Marsden and Marjorie McCracken. *The Hopf bifurcation and its applications*, volume 19. Springer-Verlag, 1976.

[11] Michael L. Rosenzweig and Robert H. MacArthur. Graphical representation and stability conditions of predator-prey interactions. *The American Naturalist*, 97(895):209–223, 1963.

[12] Gunog Seo and Gail S.K. Wolkowicz. Sensitivity of the dynamics of the general Rosenzweig-MacArthur model to the mathematical form of the functional response: a bifurcation theory approach. *Forthcoming Manuscript*.

[13] Gunog Seo and Gail S.K. Wolkowicz. Sensitivity of the dynamics of the general Rosenzweig-MacArthur model to the mathematical form of the functional response: a bifurcation theory approach. *Journal of Mathematical Biology*, 2016.

[14] Hal L. Smith and Paul Waltman. *The Theory of the Chemostat: Dynamics of Microbial Competition*. Cambridge University Press, 1995.

[15] Gail S.K. Wolkowicz and Zhiqi Lu. Global dynamics of a mathematical model of competition in the chemostat: general response functions and differential death rates. *SIAM Journal on Applied Mathematics*, 52(1):222–233, 1992.